agriculture

MDPI

Article

High-Efficiency Photovoltaic Equipment for Agriculture Power Supply

Olga Shepovalova *, Andrey Izmailov, Yakov Lobachevsky and Alexey Dorokhov

Federal Scientific Agroengineering Center VIM, 1-St Institutskiy Proezd, 5, 109428 Moscow, Russia
* Correspondence: shepovalovaolga@mail.ru; Tel.: +7-906-092-95-60

Abstract: Developing an energy supply based on resources whose use does not spoil the noosphere and the creation of such energy supply of efficient equipment whose operation does not cause any damage to nature and man is an urgent task. The need for such an approach is especially relevant and noticeable in agriculture. This article presents the final results of complex studies of new PV devices and PV systems based on them. Considered in the article are the best solutions we propose to improve PV equipment and make it more attractive for agricultural consumers. The developed vertical and planar high-voltage multijunction silicon PV cells and PV modules on their basis are presented. The first type of modules have a maximum power point voltage of up to 1000 V, specific power of up to 0.245 ± 0.01 W/cm^{2,} and efficiency of up to 25.3% under a concentration ratio range of 10–100 suns. The samples of the second module type (60,156.75 × 156.75 mm PV cells) have an open-circuit voltage of 439.7 V, a short-circuit current of 0.933 A, and a maximum power of 348 W. Additionally, two types of newly designed solar energy concentrators are described in this article: one-dimensional double-wing concentrator ensuring low Fresnel optical losses and multi-zone parabolotoric microconcentrator with the uniform radiation distribution in the focal region, as well as modules based on these concentrators and the developed PV cells. For PV modules, the maximum power degradation is 0.2–0.24% per year in a wet ammonia environment. For concentrating PV modules, this degradation is 0.22–0.37% per year. This article sets out the principles of increasing the efficiency of PV systems by increasing the level of systematization and expanding the boundaries of PV systems. The thus-created PV systems satisfy 30–50% more consumer needs. Thanks to a higher output voltage and other specific features of the developed modules, PV system loss decreased by 12–15%, and maintenance losses also decreased.

Keywords: green energy supply; agricultural electrification; high-efficiency photovoltaic equipment; complex energy supply systems

Citation: Shepovalova, O.; Izmailov, A.; Lobachevsky, Y.; Dorokhov, A. High-Efficiency Photovoltaic Equipment for Agriculture Power Supply. *Agriculture* **2023**, *13*, 1234. https://doi.org/10.3390/agriculture13061234

Academic Editor: Massimo Cecchini

Received: 19 December 2022
Revised: 22 May 2023
Accepted: 25 May 2023
Published: 12 June 2023

1. Introduction

One of the main ways to overcome the negative impacts of modern industrial civilization is the transition to maximum harmonization with nature, which is especially topical and noticeable in the countryside [1]. The energy supply based on the resources whose use does not spoil the noosphere and the creation of such energy supply of efficient equipment whose operation does not cause any damage to nature and man is one of the mechanisms of environmental restoration. The resource for this is, first of all, solar energy [2–6].

The transition to the use of renewable energy resources is the most obvious and justifiable in agriculture. Photovoltaic (PV) systems are one of the best equipment options for specified purposes, especially considering the development of building-integrated photovoltaics (BIPV) and agrivoltaics (AgriPV).

For agriculture and rural areas, the use of photovoltaic solar energy conversion is especially topical because of the following factors [7–9]:

(1) Agriculture has the most opportunities for implementing the optimal variants of PV systems;
(2) Rural territories generally suffer from a greater constant shortage of electric power;
(3) In power supply to agricultural consumers, the inefficiency of improperly designed systems is more obvious, and such systems have a more substantial impact on life activity.

At the same time, the power supply to agriculture imposes special requirements for PV equipment, namely requirements associated with the impact of aggressive environments, e.g., ammonia, thermal and humidity conditions, etc., as well as special requirements for safety, ecological compatibility, and aesthetics. Agriculture is more sensitive to changes (increases) in the equipment cost.

In order to implement power supply in rural areas, first of all, through the application of solar energy resources and expansion of the scale of agricultural power supply with the use of PV systems, it is necessary to increase the efficiency of PV systems and make them more attractive for consumers. At present, the solutions to this problem are as follows:

(1) Efficiency enhancement of solar energy conversion is achieved through improvement in the design of PV devices and manufacturing technology (i.e., the efficiency of PV cells, concentrators, and modules), reduction in the degradation of PV devices' characteristics over time, and the enhancement of devices' resistance to environmental factors. This ensures an increase in the energy output and a minimization of the occupied space [10–14].
(2) A combination of functions (i.e., BIPV, AgriPV, etc.) ensures that there will be no need for a separate space on the land's surface for placing PV modules, in addition to cost reduction and improved aesthetics [15,16].
(3) An increase in the level of systematization, expansion of the boundaries of PV systems, and their development as complex systems ensure a reduction in losses and a higher level of consumer satisfaction [17].
(4) The placement of PV systems at the consumption site ensures the organization of energy supply based on an analogy with nature, a reduction in costs, and additional opportunities for the implementation of the first three factors mentioned above [7].
(5) An increase in the diversification of efficient PV equipment for various operational conditions enhances the PV systems' versatility and expands their application possibilities.

The overall purpose of our many years of research is to increase PV equipment efficiency at all levels [18], including PV cells, PV modules, and PV systems, thus considerably increasing the possibilities of using PV systems in agriculture.

At present, more than 90% of industrial-grade PV cells are PV cells fabricated on a silicon wafer with a *p*–*n* junction unit, which is due to their substantial advantages over any other types of PV cells (e.g., relatively low cost, accessibility and abundance of silicon, acceptable output characteristics and properties of such PV cells, and well-proven technology) [10,11,13,19].

Homogeneous semiconductor PV cells on the basis of just one *p*–*n* junction can only generate voltages limited by the potential barrier height on the junction. For silicon and gallium arsenide (i.e., the best technologically investigated PV materials), this voltage is approximately 0.6 V to 0.9 V under nonconcentrated solar radiation. At the same time, most typical electronic devices require considerably greater voltage levels for their operation. When using single-junction PV cells for obtaining the required values of voltage, one has to connect a sufficiently large number of cells/modules in series, which results in power loss due to contact resistance and non–uniformity in the parameters of individual cells/modules. Additionally, it leads to a reduction in efficiency and sturdiness against external factors. The typical planar crystalline silicon PV modules (60 mono-Si PV cells with single *p*–*n* junction and with a size of 156.75 × 156.75 mm) have an open-circuit voltage ($V_{o.c}$) of 44 V and a short-circuit current ($I_{s.c}$) of 9.5 A, and their voltage and current at the maximum power point are 36.3 V and 8.8 A, respectively. The required voltage and power values of a PV array based on traditional PV modules are usually provided at sufficiently high DC values. Reducing these values can significantly reduce ohmic losses and therefore will

both increase the efficiency and reliability of PV systems and reduce costs. Moreover, such PV modules occupy quite a great area [10–13,19–22]. However, in agriculture, limitations generally exist for the placement of PV modules and, as mentioned above, have more stringent requirements for immunity to environmental factors and cost.

Based on this, the first task of our research was to develop high-voltage silicon PV cells that would enable a significant increase in the output voltage of PV equipment and overcome other disadvantages of conventional PV modules that limit the PV equipment used for agriculture power supply.

Earlier on, research was pursued to develop high-voltage vertical multi-junction Si PV cells for space applications [23]. These cells had acceptable efficiency only when the concentration was 1000 suns or higher, and they were not convenient for terrestrial applications. More recent studies also refer to cells operating under high concentrations (efficiency of up to 19% under 2480 suns), which have also not been applied in terrestrial photovoltaics [24]. Terrestrial high-voltage vertical multi-junction Si PV cells suitable for mass application were, for the first time, proposed and developed in the course of the studies summarized in this paper.

Considering the fact that mass technologies are oriented toward the production of planar PV modules and also that the components of PV systems (mass design solutions), such as PV plants, BIPV, and AgriPV, are designed on the basis of the conventional planar PV modules, planar high-voltage silicon PV cells are required. Making such cells was a new idea. Our ideas and theoretical studies were presented in [25–30]. Besides increasing the output voltage, these cells had to accomplish the objective of creating high-voltage PV modules with dimensions matching the standard dimensions of the mass-produced crystalline Si PV modules. Additionally, such modules should be manufactured with the maximum use of existing equipment.

The higher the concentration of the solar energy arriving at radiation receivers (RRs) is, the higher the photoelectric conversion efficiency is. The use of concentrators enables an increase in the irradiance of the active surface of PV cells and therefore increases the efficiency of PV modules/PV systems [11,14,31,32]. A review of the current state of concentrator applications in photovoltaics is presented in [32–36]. Two types of solar radiation concentrators were of interest in terms of developing highly efficient concentrator photovoltaic (CPV) modules: focon-type concentrators and concentrators containing a symmetrical reflecting surface (RS) fabricated as a chute (compound parabolic concentrators). Concentrators of these types have the following important advantages, compared with other types of concentrators: (1) a long daily operation period within the parametric angle of the concentrator without tracking the sun; (2) the possibility of using diffuse radiation, thus increasing the amount of the total irradiance coming to the concentrator aperture, by up to 20%. The mirror RS on the current technological horizon may have a reflection coefficient of 99% or more, which sets this mirror concentrator apart from lens-based ones.

The main disadvantage of concentrators manufactured in the form of solids of revolution, including focon types, and other toroids, as well as concentrators based on Fresnel lenses, is a nonuniform distribution of irradiance intensity over the active surface of RRs. This results in a decrease in efficiency because PV converters are most efficient when irradiance is uniform. Compound parabolic concentrators have uniform radiation density in the rectangular focal region. The main problem of such concentrators is that the rays reflected from the part of RS located close to the focal plane fall on the active surface of RRs at high angles. This results in a sharp increase in the coefficient of radiation reflected from the active surface of RRs (Fresnel losses) [14,36–39].

Moreover, all of the operated efficient PV systems based on CPV modules are bulky and have incomparably larger dimensions and weights than those based on traditional planar PV modules. They require complex and insufficiently reliable tracking systems. This, to a large extent, brings to naught their advantage of a higher performance factor. In addition, naturally, this makes them hardly applicable in agricultural power supply systems.

Free from these defects are CPV modules based on microconcentrators whose dimensions are comparable to those of conventional planar PV modules. The best results in implementing microconcentrators are presented in [40–42]. There is a considerable problem associated with the unevenness of RR illumination while using mirror concentrators, which may be reduced by optimizing the form of RS, and there is also a problem of inherent losses caused by absorption when Fresnel lenses are used [36,39].

In certain situations, the use of toroidal concentrators is the most effective. In [43], we presented a series of newly developed semitoroidal concentrators.

Another task of our research was to remove/minimize the previously mentioned defects of focon-type concentrators and compound parabolic concentrators and to design efficient CPV modules on the basis of the developed concentrators and high-voltage multijunction cells.

The aim of this article was to present the final generic research results that yielded real practical outcomes, starting from scientific ideas to operating devices and installations. Schematically, the reviewed studies are outlined in Figure 1. The results presented in the paper include two types of high-voltage PV cells (Section 2), optimized solar concentrator structures (Section 3), and four types of PV modules on their basis (Sections 2 and 3). As well, this article presents research on the development of more efficient PV systems by increasing the level of systematization and expanding the boundaries of PV systems. The final efficiency of such systems is evaluated by the degree of consumer need satisfaction (Section 4). To date, the results of our theoretical studies related to PV cells and concentrators have mainly been published. The research results of fabricated PV cells, concentrators, and modules on their basis, are published for the first time in this article. For the time being, quite a high correlation between theoretical calculations and the operating characteristics of real instruments was achieved, which enabled us to present the relevant results in this manuscript.

When proposing the ideas related to the development of PV devices (Sections 2 and 3), along with efficiency improvement, a task was set to minimize the costs at the stage of the introduction of devices into production (by minimizing changes in the manufacturing technology) and at the stage of the creation of PV systems based on the developed PV and CPV modules (by minimizing changes in the technology and design of PV systems and mating structures). These aspects were indispensably taken into account when analyzing and choosing the optimal options. The solutions to this task included the choice of silicon as the basic material for PV cells, the creation of planar high-voltage cells whose dimensions correspond to those of conventional crystalline silicon PV cells, and CPV modules whose dimensions correspond to those of traditional planar PV modules.

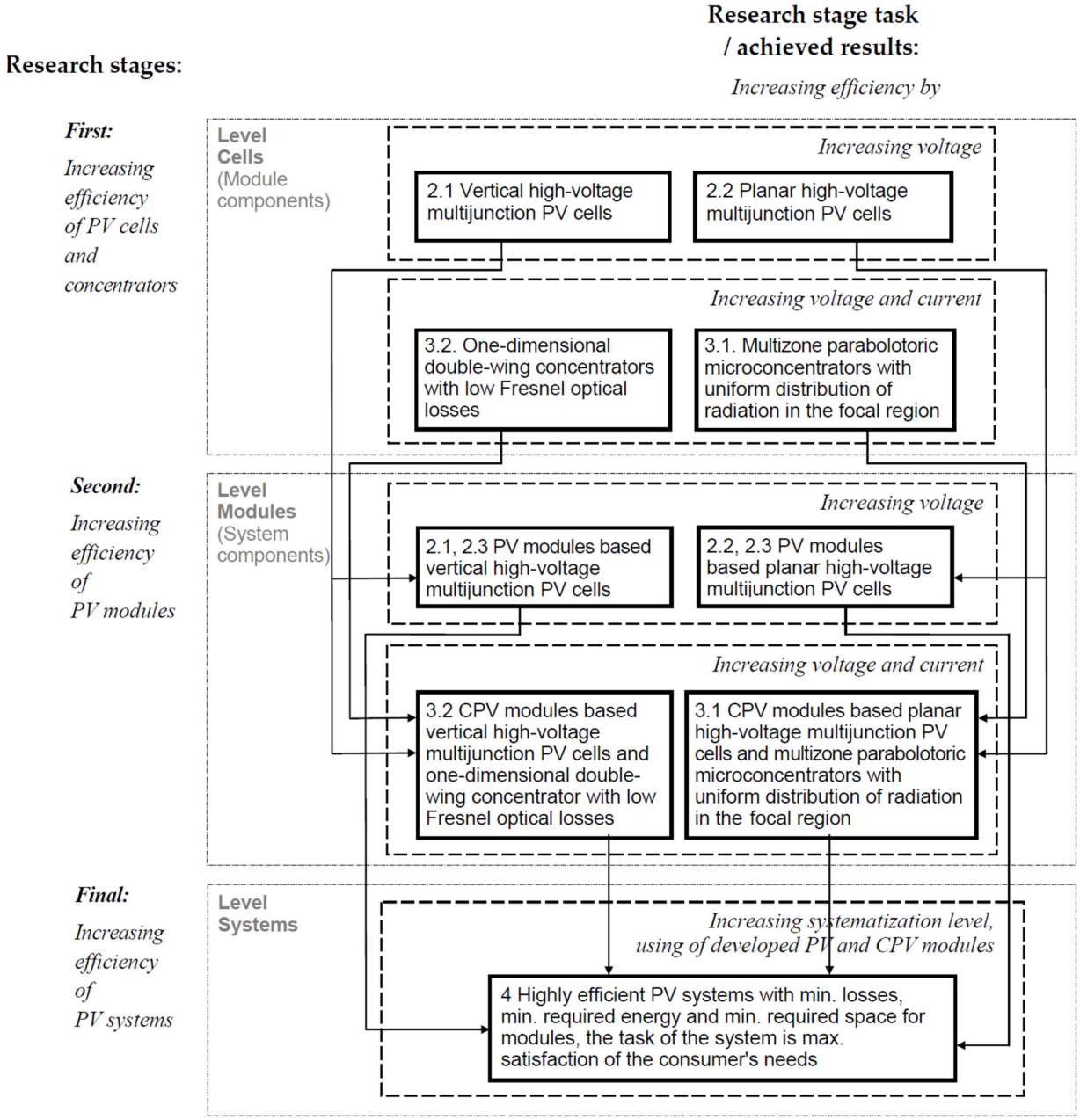

Figure 1. General scheme of research (numbers correspond to the section/subsection number in this article).

2. Increasing Energy Production by Increasing Voltage—Improvement in the Design of Photoelectric Cells

2.1. Vertical High-Voltage Multi-Junction Silicon PV Cells

Three technologies have been used to form multi-layer structures: soldering unit cells using solder plugs with diffused layers, epitaxy, and breakdown [44]. Currently, PV cells are manufactured via plug soldering with subsequent cutting into size-defined cells and the application of antireflection coating with nanoclusters to the end face (active surface) [45,46]. Figure 2a,b show the structure of a typical vertical high-voltage PV cell and a PV module composed of these cells. As one can see from Figure 2, both the cells and modules of this design are much more space-saving than those manufactured using traditional planar technology. The cell voltage is equal to the sum of the voltages of microcells (0.58–0.62 V per microcell). The efficiency achieved for the designed cells under single-fold radiation is comparable to that of conventional silicon PV cells.

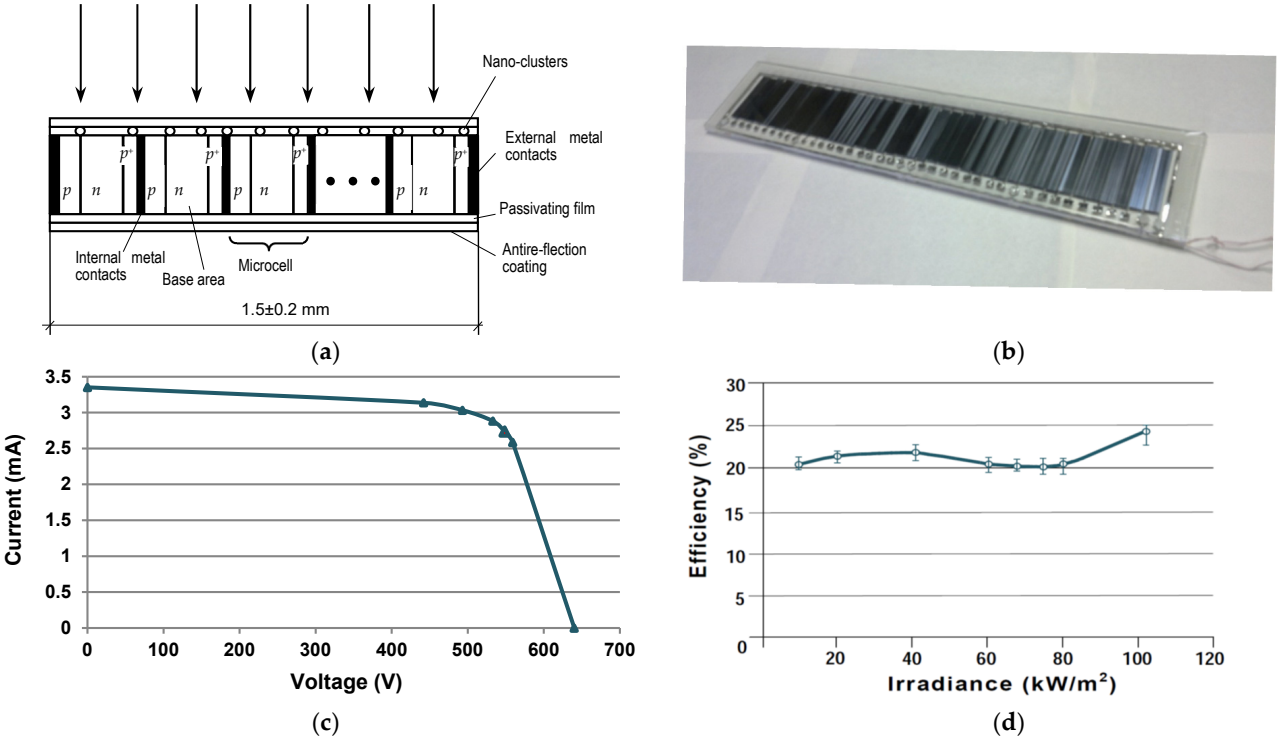

Figure 2. (**a**) PV cell structure; (**b**) PV module based on vertical multi-junction PV cells, 40 60 × 10 mm PV cells; (**c**) *I*–*V* curve of developed PV modules, 10 suns; (**d**) dependence of efficiency on irradiance.

PV cells have universality in relation to the radiation level, i.e., in contrast to traditional silicon planar PV cells, their voltage does not decrease as concentration increases. Moreover, they have low sensitivity to the radiation incidence angle.

PV modules based on vertical high-voltage multi-junction silicon PV cells have a voltage rate of up to 1000 ± 15 V at the maximum power point. For solar radiation concentration ratios ranging from 10 to 100 suns, the specific power of such modules is up to 0.245 ± 0.01 W/cm^2, and their efficiency is up to 25.3%. The modules are encapsulated with polysiloxane gels (see Section 2.3), which facilitates the extension of their expected service life up to about 50 years. The operating range of their ambient temperature is from –60 to 110 °C. The module efficiency, which is 18–22%, remains the same when the temperature rises up to 60 °C, which simplifies their cooling system while working with concentrators. The production process does not require the use of silver, screen printing, photolithography, or any other time-consuming procedure or expensive materials. Figure 2c shows the *I*–*V* curve of the developed PV module. The test conditions were as follows: direct normal irradiance of 10 × 1000 W/m^2, cell temperature of 25 °C, and spectral irradiance distribution of direct normal AM1.5. Figure 2d shows the PV module's efficiency dependence on the level of active surface irradiance [46].

The operating voltage of 1000 ± 15 V enables the use of these PV modules with transformerless inverters and connecting them to high-voltage direct-current 110–500 kV power lines without the need for converting substations. To obtain the operating voltage of 1000 V with the use of conventional planar PV modules, it would be necessary to connect more than 1800 150 × 150 mm planar PV cells in series, in which case the total length of the modules would exceed 300 m. It is also important that the operating voltage of one module can be equal to the accepted nominal DC voltage of large photovoltaic systems (system voltage), for example, solar power plants such as AgriPV systems.

The main problem involves the reproducibility of characteristics (wide spread of parameter values). Thus far, it has been impossible to achieve parameter values in the required narrow interval with the change from batch to batch.

2.2. Planar High-Voltage Multi-Junction Silicon PV Cells

The currently developed planar high-voltage silicon PV cells are multi-junction homogeneous PV structures [25–30]. The doped layers form planar diodes n^+–p–p^+ (p^+–n–n^+; n–p–p^+; p–n–n^+) or n–p microstructures (unit cells) connected in series in the direction of radiation propagation. Figure 3 shows the design options of planar high-voltage PV cells, while Table 1 presents the advantages, design specificity, and technological features borrowed from PV cells of various types in order to develop planar high-voltage multi-junction PV cells.

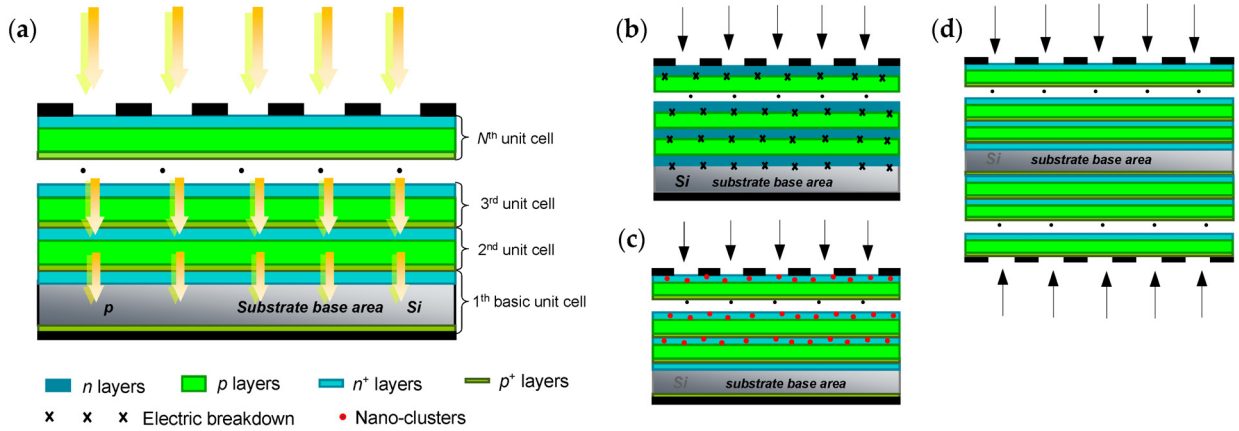

Figure 3. (**a**) High-voltage planar PV cells with basic option; (**b**) structure manufactured using the electric breakdown technology; (**c**) structure with nanoclusters; (**d**) bifacial structure.

Table 1. Advantages, specificity of design, and technologies borrowed from various types of PV cells to develop high-voltage planar multi-junction PV cells.

PV Cell Type	Advantages, Specificity of Design, and Technology
Conventional planar	Dimensions Basic complete processing lines Consequent designs Preferable direction of radiation adsorption
Silicon multi-junction	High output voltage Ability to operate under concentrated solar radiation Low electric losses
III-V-based multi-junction	Multilayer design Layer preparation technology, interconnection via tunnel junctions Layer thickness
Silicon-based thin film	Layer thickness

The small ($\leq$10 μm) thickness of layers and, consequently, unit cells make them practically transparent considering solar radiation. Each unit cell receives radiation that consecutively passed through the previous semiconductor layers. The thickness of the base unit cell area does not exceed the diffusion length of minority charge carriers.

The theoretical and most of the experimental parts of this research were carried out using the basic option of the design, as shown in Figure 3a. The basic option of PV cells was fabricated through the use of epitaxy by transferring epitaxial layers to the basic unit cell (silicon wafer with a p–n junction formed via diffusion). The first basic unit cell ensures the mechanical strength of the entire structure. As the p^+ and n^+ layers are heavily doped, a conductive contact occurs between them owing to the quantum-mechanical effect of tunneling through the p^+–n^+ junction. The dimensions of PV cells are determined by the dimensions of the wafer and correspond to the dimensions of traditional crystalline Si PV cells.

The thickness of p, n, and n^+ layers is from 12 nm to 9.8 μm, while that of p^+-type layers is from 10 nm to 120 nm. The concentration of active impurity in thin heavily doped p^+-type layers is more than 10^{19} cm^{-3}. In general, the thickness of layers increases with the distance from the active surfaces, which enables the production of PV cells with the required output parameters and their nonsignificant distribution with a wide tolerance for layer identity. The number of layers is determined based on equipment capability and the specifics of the layer formation process, as well as the expediency of using solar cells with a specific number of layers in the PV modules.

To avoid losses in the circuit, each unit cell must operate under radiation at its optimal point of the volt–ampere characteristic, which means the equality of the photogenerated currents flowing through the unit cells:

$$\begin{cases} \int\limits_0^\infty \frac{d\Phi}{d\omega} \cdot e^{-\alpha \sum\limits_{k=i+2}^{N} d_k} \cdot \left(1 - e^{-\alpha d_{i+1}}\right) \cdot d\omega = \int\limits_0^\infty \frac{d\Phi}{d\omega} \cdot e^{-\alpha \sum\limits_{k=i+1}^{N} d_k} \cdot \left(1 - e^{-\alpha d_i}\right) \cdot d\omega;\ i = 2,3,\ldots,N-1 \\ \int\limits_0^\infty \frac{d\Phi}{d\omega} \cdot e^{-\alpha \sum\limits_{k=i+1}^{N} d_k} \cdot \left(1 - e^{-\alpha d_i}\right) \cdot d\omega = \int\limits_0^\infty \frac{d\Phi}{d\omega} \cdot e^{-\alpha \sum\limits_{k=2}^{N} d_k} \cdot Q_i(\omega) \cdot d\omega; \quad i = 2,3,\ldots,N \end{cases} \tag{1}$$

where Φ is the incident photon flux; α is the radiation absorption coefficient depending on photon frequency ω or wavelength λ and on the nature of the semiconductor; d_k and d_i are the thickness of the k-th or i-th unit cell, respectively; $Q_i(\omega)$ is the spectral charge carriers collection efficiency for the p–n junction in the i-th unit cell; and N is the number of unit cells in an entire PV cell.

The requirement of Equation (1) is met by determining the optimal values of the thickness of each unit cell as follows:

$$d_i = \frac{1}{\alpha} \ln \frac{1 - e^{-2\alpha\delta} + Q_i e^{-\alpha\delta}\left(1 - e^{-2\alpha\delta(i-1)}\right)}{1 - e^{-2\alpha\delta} + Q_i e^{-\alpha\delta}\left(1 - e^{-2\alpha\delta(i-2)}\right)};\ i = 2,3,\ldots,N \tag{2}$$

where $\alpha\delta$ is the complex optical–technological parameter of the PV cell.

The density of the photocurrent generated in the i-th unit cell is subject to light absorption in the previous layers.

$$J_{\mathrm{ph}i} = q\Phi_0 S_i(\alpha, \xi);\ i = 1,\ 2,\ \ldots, N \tag{3}$$

where q is the absolute value of the electron's charge, Φ_0 is the incident photon flux density, S_i is the spectral charge carriers collection efficiency (photoresponse) of the i-th unit cell, and ξ is the angle of radiation incidence onto the active surface.

Volt–ampere characteristic is expressed as follows:

$$V = \frac{AkT}{q} \sum_{i=1}^{N} \ln\left(\frac{\left(\frac{q\Phi_0 \cdot Q_i}{1+(N-1)\cdot Q_i} - J_{\mathrm{ph}}\right)}{J_{0i}} + 1\right) \tag{4}$$

where A is the parameter of characteristic curvature, k is the Boltzmann constant, T is the cell temperature, and J_{0i} is the reverse dark current density in the i-th unit cell.

The collection efficiencies of spectral charge carriers of unit cells are determined as follows:

$$\begin{gathered} S_1(\alpha, \xi) = S_{\mathrm{b}}(\alpha, \xi) = \cos\xi \cdot e^{-\frac{\alpha}{\cos\vartheta}\left(\sum\limits_{k=2}^{N} d_k + 2\delta(N-1)\right)} \cdot Q_{\mathrm{b}}(\alpha, \vartheta) \\ S_i(\alpha, \xi) = \cos\xi \cdot e^{-\frac{\alpha}{\cos\vartheta}\left(\sum\limits_{k=i+1}^{N} d_k + 2\delta(N-i)+\delta\right)}\left(1 - e^{-\frac{\alpha}{\cos\vartheta} d_i}\right);\ i = 2,\ \ldots, N-1 \\ S_N(\alpha, \xi) = \cos\xi \cdot e^{-\frac{\alpha}{\cos\vartheta}\delta} \cdot \left(1 - e^{-\frac{\alpha}{\cos\vartheta} d_N}\right) \end{gathered} \tag{5}$$

where Q_b is the collection efficiency of the charge carriers in the basic cell, ϑ is the refraction angle in a semiconductor structure, and δ is the thickness of the tunnel layer in the unit cells (the difference between the tunnel layers of unit cells can be neglected).

Angle ϑ is determined using the relation $\sin\xi = n \cdot \sin\vartheta$, where n is the radiation refraction index in the semiconductor. Angle ξ is equal to 0° when the rays are perpendicular to the active surface. The reverse dark current density in the i-th unit cell, given the uniform technology used in the fabrication of unit cells, does not depend on the unit cell number, i.e., $J_{0i} = J_0$, as evident from Equation (1).

The plots showing the main characteristics of the developed high-voltage multi-junction PV cell with the basic structure (see Figure 3a) and different unit cell numbers are presented in Figure 4. The characteristics of the final experimental samples quite accurately correspond to the results of computer simulations and calculations.

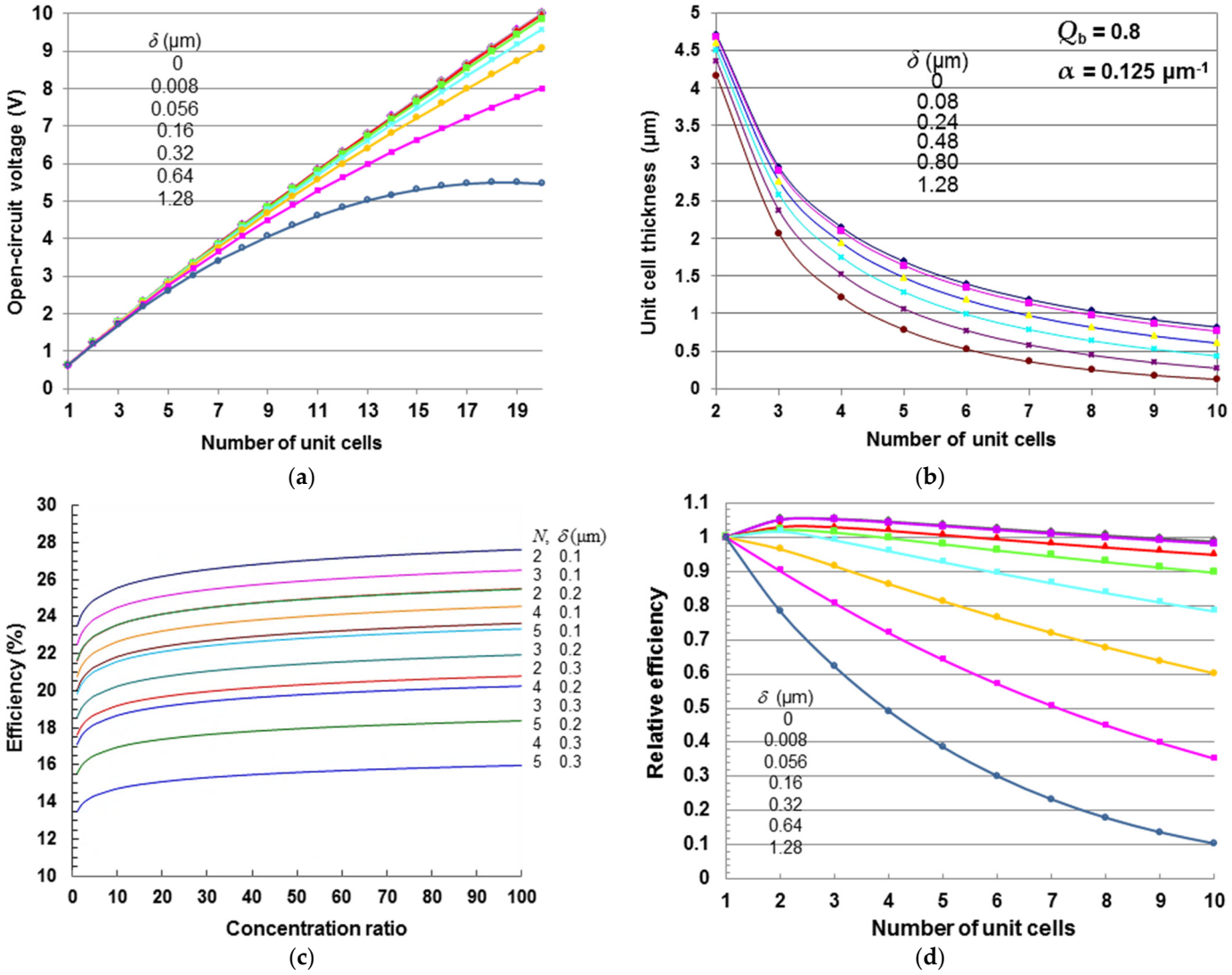

Figure 4. (**a**) Open-circuit voltage of high-voltage planar PV cells under solar radiation, $a = 0.125\ \mu m^{-1}$, A = 2, $J_0 = 10^{-7}$ A/cm^2, and $q\Phi = 45$ mA/cm^2; (**b**) dependence of the optimum unit cell thickness on it number; (**c**) dependence of efficiency on solar radiation concentration; (**d**) relative efficiency, $a = 0.125\ \mu m^{-1}$, A = 2, $J_0 = 10^{-7}$ A/cm^2, and $q\Phi = 45$ mA/cm^2.

For the experiments, PV cells (see Figure 3a) were originally fabricated using the basic design option with the number of unit cells N from 1 (only the basic unit cell without epitaxy layers) to 20 (see Figure 4a). For technological reasons, more detailed research was

carried out to determine the characteristics of unit cells using samples with $N = 2$, $N = 5$, and $N = 10$.

The dependence of the open-circuit voltage of PV cells on N is shown in Figure 4a, for various values of tunnel layer thickness δ for $\alpha = 0.125\ \mu m^{-1}$, $Q_b = 0.8$, a radiation intensity equal to that of solar radiation ($q\Phi = 45\ mA/cm^2$), and for other parameters corresponding to the recombination current mechanism ($A = 2$; $J_0 = 10^{-7}\ A/cm^2$). The open-circuit voltage increases monotonically with N (growing almost linearly for small values of N), weakly depending on the values of J_0 and Q. In the asymptotic limit, for $N \cdot Q >> 1$, it becomes dependent on N, to an extent that is weaker than the linear law and does not change for any value of Q.

As seen from Equation (2), the optimal thickness d_i decreases in inverse proportion to the radiation absorption coefficient α, logarithmically reduces as the unit cell number i increases, and increases as the collection efficiency of charge carriers Q_b increases in the first basic unity cell. The dependence of the optimal thickness of a unit cell on its number for various values of δ is shown in Figure 4b. PV cells may operate under concentrated radiation without a noticeable decrease in voltage, and they have low sensitivity to the solar radiation incidence angle. The efficiency of PV cells does not exceed the maximum efficiency of the basic unit cell only for small values of the tunnel layer thickness δ. For a given value of radiation absorption coefficient α, this thickness, layer number N, and the relevant value of open-circuit voltage must not exceed the corresponding limiting values. For example, for $\alpha = 0.125\ \mu m^{-1}$, there must be $\delta \leq 0.16\ \mu m$, $N \leq 9$, and $V_{o.c} \leq 4.5$ V. A sharp drop in PV cell efficiency was observed if $\delta \geq 0.32\ \mu m$.

Experimental samples of PV modules were manufactured from 60 PV cells with a size of 156.75 × 156.75 mm with $N = 10$. The PV cells were connected in a series–parallel comprising two strings of 30 cells each or in series. The modules were encapsulated using polysiloxane gels (see Section 2.3). Figure 5a shows the module during testing. Additionally, Figure 5b shows the averaged I–V curve of the developed modules under the standard test conditions (STC) (cell temperature of 25 °C, irradiance of 1 sun, i.e., 1000 W/m^2, and spectral irradiance distribution of AM1.5).

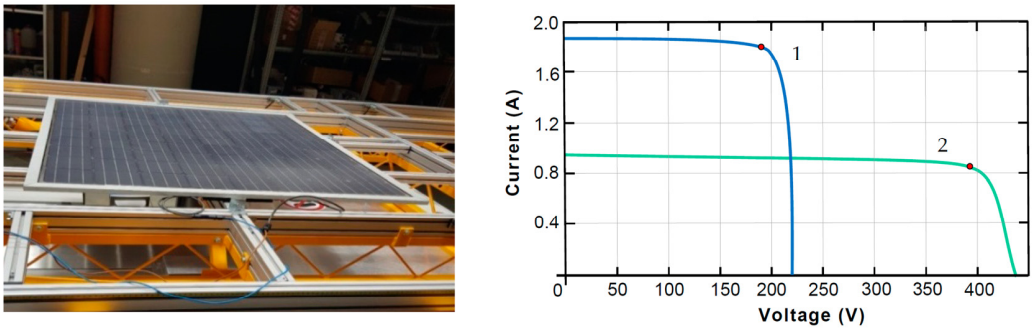

(**a**) (**b**)

Figure 5. (**a**) PV module with planar high-voltage multi-junction silicon PV cells ($N = 10$) on the test bench; (**b**) I–V curve of the developed modules at STC, $N = 10$ (curve 1—two strings of 30 cells each and curve 2—1 strings of 60 cells).

2.3. Performance Deterioration Reduction and External Impact Hardening—Improvement in PV Module Manufacturing Technology

Planar crystalline Si terrestrial PV modules manufactured using the conventional lamination technology lose up to 15–20% of their maximum power at STC after 20 years of operation in tropical climates and after 25 years of operation in temperate climates. One of the reasons for it is the degradation of optical polymeric encapsulants such as ethylene vinyl acetate (EVA) and other plastics induced by ultraviolet radiation and high temperatures [47].

High-voltage cell modules considered in Sections 2.1 and 2.2 were manufactured using polysiloxane gels instead of conventional EVA as the filling material [46,48]. The replacement of the standard encapsulant with EVA and the conventional lamination process with a silicon composition that is poured as liquid and then hardens and turns into polysiloxane gels considerably slows down the performance deterioration of such modules in time. The process reaction is as follows:

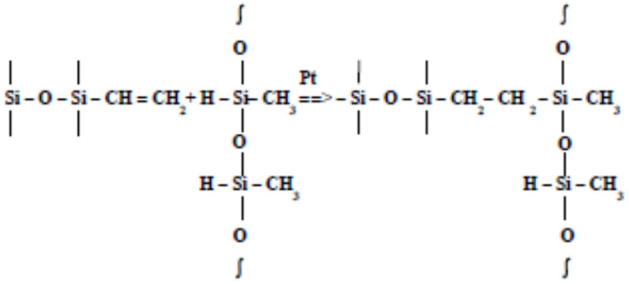

According to the laboratory test data (tests in compliance with requirements of IEC 61215-2:2021, IEC 62716:2013, IEC 61701:2020, and IEC/TS 63126:2020 [49–52]), the module's ultimate power degradation at STC was approximately 15% for 50 years. Such a result was achieved thanks to a considerably lower corrosiveness of silicon gels. Moreover, the initial output power of the modules increased thanks to higher gel transparency and a decrease in the operating temperature of PV cells. PV modules are fire-safe and have increased resistance to operation in environments with a high concentration of ammonia and in tropical and marine climates.

The comparative characteristics of modules encapsulated with polysiloxane gels and conventional silicon modules filled with EVA are shown in Table 2.

Table 2. Comparison of the characteristics of PV modules with two types of filling materials [48].

Parameter	Encapsulant	
	Polysiloxane Gels	**EVA**
Degradation of maximum power at STC (%) per year for 25 years	0.2–0.3 about 7.5	0.6–2.0 15 ÷ 20
Operating temperature (°C)	−60 to +110	−40 to +85
UV radiation durability	high	low
Refraction index	1.406	1.482
Transparency for solar radiation (%)		
λ = 360 nm	90	8
λ = 400 nm	92	62
λ = 600 ÷ 1000 nm	93	91
Corrosive agents		
during encapsulation	none	acetic acid
during operation	none	acetic acid
Mechanical stress		
during encapsulation	no	yes
during operation	no	yes
Modulus of elongation (N/mm^2)	0.006	10.0
Linear coefficient of thermal expansion ($10^{-4} \cdot K^{-1}$)	2.5	4.0

The encapsulation technology ensures a reduction in costs thanks to higher operational characteristics of modules (higher resistance to aggressive environments, e.g., in environments with the presence of ammonia in the ambient air, high humidity, etc., which are characteristic of various agricultural facilities), along with a considerable decrease in the degradation of these characteristics.

3. Increasing Energy Production by Increasing Voltage and Current per Unit Area of Cell Active Surface—Concentrator Design Improvement

In the course of our studies, we sought to optimize the form of the RS of both focon-type and compound parabolic concentrators. In the case of focon-type concentrators, it was important to solve the problem of nonuniform radiation distribution over the RR's operating surface, while in the case of compound parabolic concentrators, we had to minimize Fresnel losses. As a result, two types of effective CPV modules were built: the first based on focon-type concentrators and planar high-voltage cells, and the second based on compound parabolic concentrators and vertical high-voltage cells. The designs were based on the conditions that the concentrators should have such dimensions that would lead to comparable dimensions of the resulting CPV modules to those of conventional crystalline silicon PV modules, and that CPV modules could be used in individual power supply systems. Additionally, the design of CPV modules should match the components of mass-produced PV systems as much as possible.

3.1. Multi-Zone Parabolotoric Microconcentrators with Uniform Radiation Distribution in the Focal Region

The reflecting surface of the developed multi-zone solar radiation microconcentrators was formed via the rotation of a certain curve (generatrix) around a symmetry axis that does not cross this curve and passes through the focal spot center. A microconcentrator with an internal mirror RS operates on the principle of collecting the reflected rays into a circular focal region.

Figure 6 shows examples of a single-zone concentrator and a five-zone concentrator, as well as the outlay of a finished concentrator with high-voltage planar PV cells (see Section 2.2).

The RS of a microconcentrator is composed of several zones lying one above another. The RS generatrix constitutes several smoothly merging parabolas each of which forms a separate zone. Each zone has the form of an axisymmetric solid with a symmetry axis that coincides with that of the concentrator. Each zone of the RS ensures a homogeneous reflected radiation distribution over the entire focal region, and the number of reflected rays incident on each point of the concentrator's focal region is equal to the number of zones (see Figure 6d). At the same time, the form of the RS meets the condition of minimizing the incident angle for rays reaching the RR's active surface.

The general system of equations describing the RS profile is as follows:

$$\begin{cases} \left(\frac{dx_i}{dy_i}\right)^2 + \frac{2y_i}{x_i - z_i} \cdot \frac{dx_i}{dy_i} = 1;\ i = 1, 2, \ldots, N \\ x(y_i - 0) = x(y_i + 0);\ x_i \in [r_i; R_i];\ R_i = r_{i+1} \text{ at } i = 1,\ 2, \ldots, N-1 \\ x_1 = r_1 \ \text{ at } \ y_1 = 0 \\ \lim\limits_{y \to y_i - 0} \frac{dx}{dy} = \lim\limits_{y \to y_i + 0} \frac{dx}{dy} \\ \sum\limits_{i=1}^{N} \left| \frac{x_i dx_i}{z_i dz} \right| = \sum\limits_{i=1}^{N} K_i \\ K = 1 + \sum\limits_{i=1}^{N} K_i;\ K_i = \frac{{R_i}^2}{{r_i}^2};\ K = \frac{{R_N}^2}{{r_1}^2} \end{cases} \quad (6)$$

where, as shown in Figure 6a, x_i is the current position of the point of ray arrival at the i-th zone on the X axis; x_i is equal to the radius of a section of the RS by the plane that is perpendicular to the concentrator's rotation axis and passes through the point y_i ($r_i \leq x_i \leq R_i$); y_i is the current position of the point of ray arrival at the i-th zone on Y axis coinciding with the concentrator's rotation axis; z_i is the position of the point of arrival of the ray reflected from the i-th zone at the focal spot on the X axis ($-r_i \leq z_i \leq r_i$); K_i is the concentration ratio in the focal region ensured by the i-th zone of the RS; K is the total concentration ratio in the focal region; N is the number of zones; and r_i and R_i are the

radiuses of the smallest and largest sections of the *i*-th zone's RS, which are perpendicular to the concentrator's rotation axis.

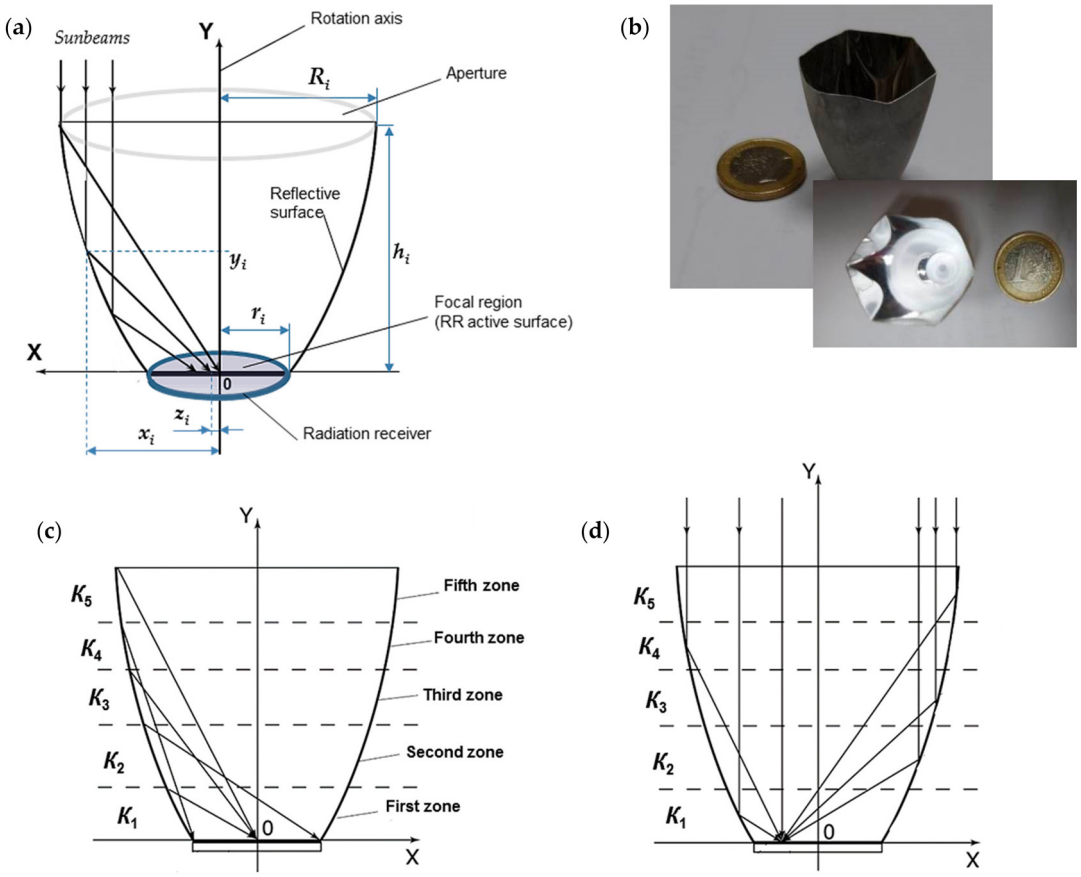

Figure 6. (**a**) Example of a single zone design; (**b**) five-zone microconcentrator with planar high-voltage PV cells corresponding to Figure 6c,d; (**c**) beam path diagram for the uppermost points of each zone, in the five-zone microconcentrator (the first zone corresponds to Figure 6a); (**d**) beam path diagram, for beams falling onto one point of RR, in the five-zone microconcentrator shown in Figure 6c.

The equations for various options of the microconcentrator design are defined in [53].

There are four options for single zones in accordance with the four possible variants of ray paths in the concentrator [53]. The microconcentrator RS is formed via the alternation of four variants of single zones. For instance, the concentrator shown in Figure 6b–d begins from a zone that is similar to that shown in Figure 6a. Then, three more zones are added where the reflected ray consequently arrives from the uppermost point of the zone at the RS center or periphery. Additionally, the fifth zone is the same as the first zone but with different values of *r*, *R*, and *h*. Each zone of the microconcentrator exposes the focal plane to light with concentration ratios K_1, K_2, K_3, K_4, and K_5, respectively. Generally, the concentration ratio of each zone K_i is distinct.

The greater the number of the zone is, the lower the reflection from the RR's active surface, and the higher the efficiency; however, this also results in a larger concentrator height.

The concentrator size depends on the size of the focal region/active surface of the RR. The smaller the focal region is, the smaller the concentrator's dimensions would be. Its size may be reduced to a very small size by using the developed PV cells, which are quite serviceable with millimeter dimensions and may be determined based on the convenience of assembly of the relevant module. The weight characteristics will be only determined by the concentrator wall thickness. The concentrators have to be capable to bear their own

weight plus the weight of protective coatings used against the impact of the environment (sealing glasses or clear plastics).

The microconcentrators and PV cells as RR are used to assemble CPV modules with the dimensions of traditional planar PV modules on the basis of crystal silicon and may be employed instead of them without material changes in the design and equipment of PV systems.

Experiments were carried out with two-zone, three-zone, and five-zone mirror microconcentrators with $2r$ = 10 mm and K = 10. The construction height of the experimental samples ranged from 26.47 mm to 36.41 mm depending on the increase in the portion of concentration accumulated in the middle zone. With that, the average incidence angle cosine varied from 0.7307 to 0.8104.

The uniformity of the achieved concentrated radiation distribution was 98.3–98.5% all over the focal region of the samples except for the boundaries along the perimeter, with the expected concentration ratio of 10^{+}. On the periphery of the focal region (approx. 2% to 4% inward of the perimeter), a light distribution inhomogeneity rate of 3% at the edge was observed. The estimated radiation distribution uniformity was 99.7%. The fact that the experimental values of the radiation distribution uniformity were lower than the estimated ones can be explained by the immaturity of the technique used to manufacture both the microconcentrators and CPV modules as a whole (i.e., the imperfect mutual adjustment of the concentrator and RR).

Furthermore, the dependence of the microconcentrator's optical efficiency on the solar ray incidence angle was not observed in the case of a planar PV cell, and this efficiency reached 0.9 with an angle of 3 degrees. The average cosine of the ray incidence angle on the focal plane, within the above limits, was greater than that for a two-zone microconcentrator, and its value was over 0.67. Such redistribution of concentrations by zones led to an increase in the eventual angles of microconcentrator disorientation, but simultaneously, the average value of the cosine of angles of ray arrival at the focal plane decreased.

The CPV modules were manufactured from five-zone samples (Figure 6b) and high-voltage planar PV cells described in Section 2.2 with a special grid (see Figure 7).

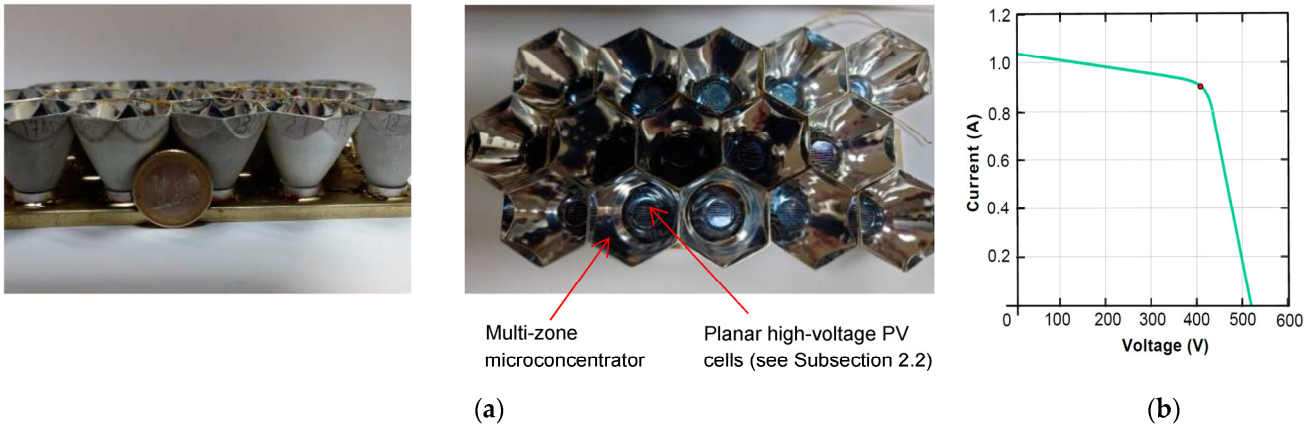

Figure 7. (**a**) CPV module in the assembly process; (**b**) *I*–*V* curve of CPV modules at CSTC.

On the concentrator RS, above the upper zone, a supplementary ring was used forming a hexagon at the ray entrance into the concentrator. This ensured that there would be no voids between the microconcentrators in the plane of the active surface. The inscribed circle diameter of the hexagon was equal to $2R_5$ = 31.6 mm. The modules consisted of 29 parallel rows with 42 microconcentrators in each. The dimensions of the module's active surface were 1607.8 × 967.4 mm, and their height was 47.2 mm. Their *I*–*V* curve at concentrator standard test conditions (CSTC) (direct normal irradiance of 1000 W/m^2,

cell temperature of 25 °C, and spectral irradiance distribution of direct normal AM1.5) is shown in Figure 7b. The efficiency change corresponds to the following equation [11]:

$$\eta_C = \eta_1(1 + \beta \ln K) \tag{7}$$

where $\beta = AkT/qV_{o.c}$ and β = 0.03–0.07.

3.2. One-Dimensional Double-Wing Concentrator with Low Fresnel Optical Loss

The body of the developed concentrator (Figure 8) was similar to that of a compound parabolic concentrator with a mirror internal RS operating on the principle of collecting the reflected rays into a rectangular focal region. The proposed principle of reducing Fresnel losses caused by radiation reflection from the RR's active surface involves minimizing the incidence angles for the reflected rays falling onto the concentrator focal region. For this purpose, RS has flat sections ($r \le x \le x_0$, $0 \le y \le y_0$) adjacent to the focal plane and smoothly passing into its curved surfaces ($x_0 \le x \le R$, $y_0 \le y$).

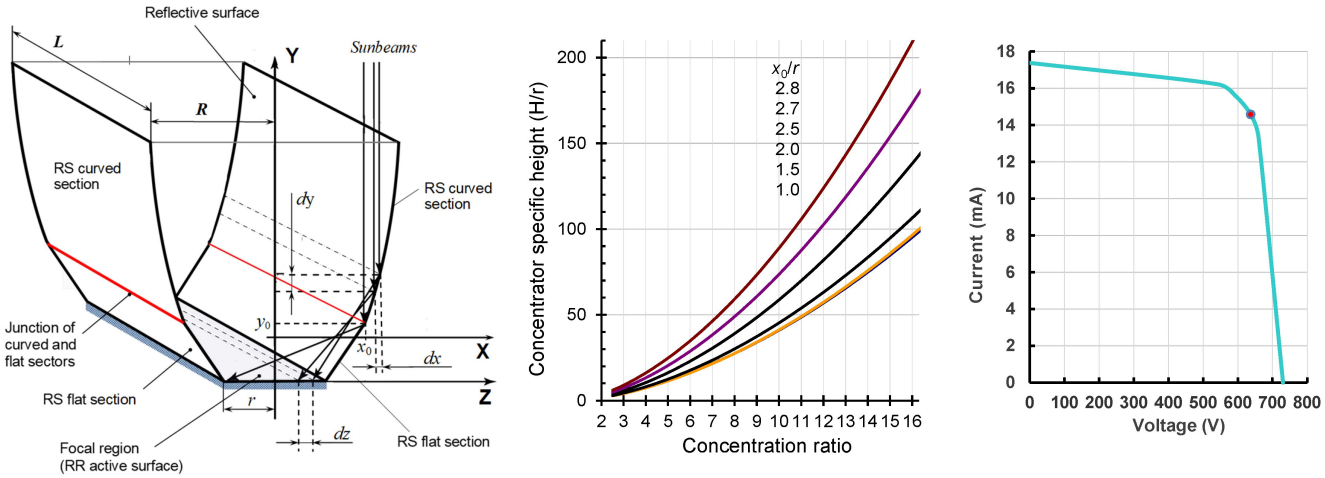

Figure 8. (**a**) Concentrator design (for the description of variables, see Equation (8)); (**b**) dependence of the concentrator specific height on radiation concentration; (**c**) *I*–*V* curve of the developed CPV module at CSTC.

The RS shape complying with the condition of uniform focal region illuminance with the maximum incidence angles value of rays falling onto the RR's active surface is described using the following set of equations:

$$\begin{cases} \left(\frac{dx}{dy}\right)^2 + \frac{2y}{x-z} \cdot \frac{dx}{dy} = 1;\ x_0 \le x \le R;\ y_0 \le y \\ \frac{dx}{dy} = \frac{x_0 - r}{y_0};\ r \le x \le x_0;\ 0 \le y \le y_0 \\ \frac{dx}{dz} = \frac{R - x_0}{2r};\ z = (x - x_0)\frac{2r}{r \cdot K - x_0} - r \\ tg\varphi = \frac{x_0 + r}{y_0} = \frac{\sqrt{(x_0 + r)(3r - x_0)}}{x_0 - r} \end{cases} \tag{8}$$

where, as shown in Figure 8a, x is the current position of the point of solar ray arrival at the RS on the X axis that is parallel with the focal plane and perpendicular to the concentrator symmetry plane ($x \ge r$); $y(x)$ is the point position on the concentrator's longitudinal symmetry plane in relation to the focal plane ($y \ge 0$); z is the position of the point of the reflected ray arrival at the focal region in relation to the concentrator's symmetry plane; x_0 and y_0 are the coordinates of the point on the junction line between the curved area ($x \ge x_0$, $y \ge y_0$) and the flat area ($r \le x \le x_0$, $0 \le y \le y_0$) of the RS ($r \le x_0 \le 3r$); K is the concentration ratio in the focal region; $2r$ is the width of the concentrator focal region

$-r \leq z \leq r$; $2R$ is the concentrator aperture size in cross-section; and $0 \leq x \leq R$ and φ is the ray incidence angle.

The shape of the concentrator's RS generatrix forms a flux of reflected radiation uniformly distributed over the rectangular focal region, thus reducing the current-spreading resistance in the illuminated layer and increasing the efficiency of solar radiation conversion into electric energy. Including flat sections in the concentrator made it possible to achieve efficient steep-wise incidence of the rays onto the focal plane at small incidence angles, resulting in a decrease in the coefficient of ray reflection from the RR's active surface. The primary important optical and energetic peculiarities of the developed product involved the symmetric property of the concentrator design, which considerably eased the requirements for the orientation towards the sun and increased the possibility of achieving high optical efficiency.

The maximum angle of the ray arrival at the RR's active surface decreased with the size of the flat horizontal section equal to $x_0 - r$. For the minimum value of $x_0 = r$, there was no flat section, and rays fell from the lower part of the concentrator at angles close to 90°, with a large reflection coefficient, while for the maximum value of $x_0 = 3r$, the incidence angle became equal to zero, and Fresnel losses were minimal. However, in this case, the size of the concentrator's flat section became unacceptably large, in a vertical direction.

The size and inclination of the flat section were chosen based on the conditions ensuring small angles of ray incidence onto the focal plane for acceptable values of the concentrator's entire height and weight. Varying this size and inclination angle enabled us to obtain a wide spectrum of concentrators ensuring target values of concentration ratios and relevant angles of radiation incidence on the focal plane.

Experiments were carried out with the concentrator option having the following parameters: r = 12 mm, $x_0 = 2r$ = 24 mm, R = 37.64 mm, and K = 10. The concentrator height was H = 75.42 mm. Modules composed of vertical high-voltage PV cells (Figure 2b) were used as RRs. For 10-fold radiation concentration, the required area of the RR's active surface decreased 10 times, and concurrently, RR efficiency increased by relatively 15–18 percent. These effects together led to a considerable reduction in cost. The chosen value of parameter $x_0 = 2r$ approximately corresponded to the optimal concentrator design in terms of the coordination of Fresnel optical losses and concentrator height, i.e., its materials content and weight. The maximum angle of ray arrival at the RR surface was $\varphi = 60°$. The concentrator ensured a uniform radiation distribution of 98.9% over the RR. At the same time, as in Section 3.1, unevenness was localized on the periphery of the RR. These areas were not above the cells without substantial losses of the RR's active surface thanks to the form of the vertical PV cells.

The height values H increased with the concentration ratio K, leading to the decrease in the angle of ray incidence on the focal region and thus reducing Fresnel optical losses. The dependence of the concentrator height related to the width of the PV module's active surface (concentrator focal region) on the concentration ratio, for concentrators having different values of the design parameter x_0/r, is shown in Figure 8b. Additionally, in Figure 8c, we can see the averaged I–V curve of one section of the developed CPV modules at CSTC. The dimensions of the RR's active surface, for one module section, are 10 × 1020 mm. The efficiency change corresponds to Equation (7).

4. Increasing Energy Production by Increasing Systematization Level—Optimization of the Power Supply Process as a Whole

It should be noted that in many recent studies on normative instruments (e.g., [54–58]) the approach to the construction concept of PV systems for individual facilities is close to the one we investigated. In [58], the consuming equipment (consumption circuit) is supposed to be a part of the PV system. Additionally, in the event that the consuming equipment would not be included in the PV system supply contract, such equipment shall be detailed in the technical documentation for the PV system. Nevertheless, the evaluation of the system was limited to that of its PV part. In [57], efficiency was assessed through

a conventional parameter called "service ratio", which rather schematically describes the relationships between the generated energy and satisfied needs. This methodology is only fit for a theoretical comparison of PV systems using this conventional parameter but not for the design process of PV systems and the efficiency assessment of real functioning systems.

The final objective of PV system operation, similar to any other power-generating equipment, is to provide the consumer with the required kind of energy in the specified and required quality.

The analysis of the process of power supply to individual facilities shows that the total losses caused by inefficient operation of power supply systems are 28–73% (see Figure 9). The average losses caused by improperly arranged power supply amount to 26% of the aggregate power losses. The losses caused by the unreliable performance of such systems as a result of their design features are 28% [6,17,59].

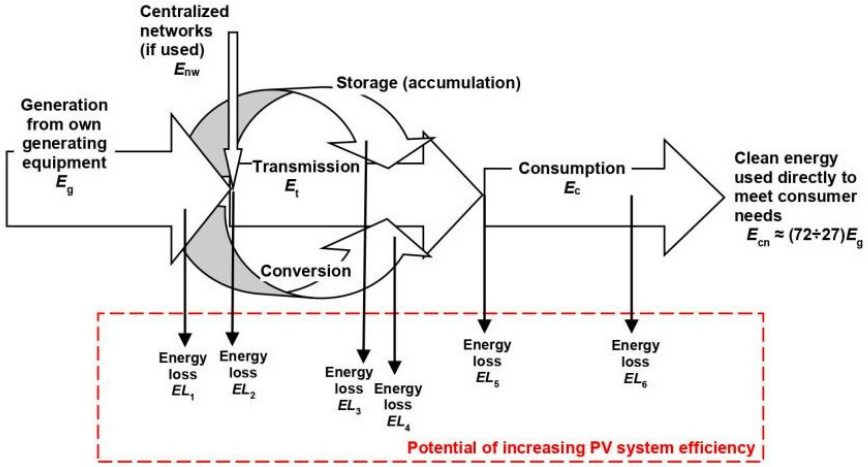

Figure 9. Diagram of the process of power supply to individual facilities.

Therefore, the actual efficiency of the power-generating equipment is determined not only by the characteristics of the generating equipment themselves, e.g., a PV system (E_g and EL_1 or $E_g + E_{nw}$ and $EL_1 + EL_2$ shown in Figure 9) but also by the peculiarities of the equipment, structures, and factors influencing the energy generation, transmission, and use processes (EL_3–EL_6). Moreover, due to the specificities of PV system functioning, even an inconsiderable change in losses (in conjunction with the time of day and of year, weather, load conditions, etc.) may substantially influence the PV system's operation and the quantity of energy delivered to the consumption points. The assembly of the above-mentioned equipment, structures, and factors, into a system and the optimization of such a system will allow for the minimization of losses, thus substantially increasing the amount of energy used by a consumer with the same output power of the PV system (both as stand-alone generating equipment and in combination with any other generating equipment and/or a network). Hence, by taking into account the final objective mentioned above, the operation of the generating equipment can become as efficient as possible.

At present, the efficiency of power supply with the use of PV systems is evaluated on the basis of their characteristics at the consuming equipment input. As seen in Figure 9, from the point of power input to the consuming equipment until the moment of meeting consumer needs, significant energy losses are possible. Accordingly, to estimate the efficiency of the PV system realistically, it should be determined based on the final result, i.e., the degree to which consumer needs are met.

This means that an increase in the PV system's efficiency can be achieved by expanding the boundaries of the system, which is mainly the new and higher level of generalization and systematization characterized by the following features:

- For power supply, a uniform complex system is created that includes all the systems, processes, and structures, involved in or influencing the power supply in any way;
- The system efficiency index is the degree to which consumer need(s) are met;
- The power supply facility (e.g., a building) is a part of the system;
- The principle of integrating functions is applied to the maximum possible extent: Each structure, technical means or subsystem shall perform as many functions as possible. When a structure (technical means, subsystem) can be built to perform the functions of several structures (technical means, subsystems), it has to be designed to combine maximum of these functions (e.g., BIPV modules);
- The development of a system begins at the time when the facility creation begins and includes a synchronized parallel interrelated development of all of the system components.

The block diagram of such a highly efficient PV system is shown in Figure 10.

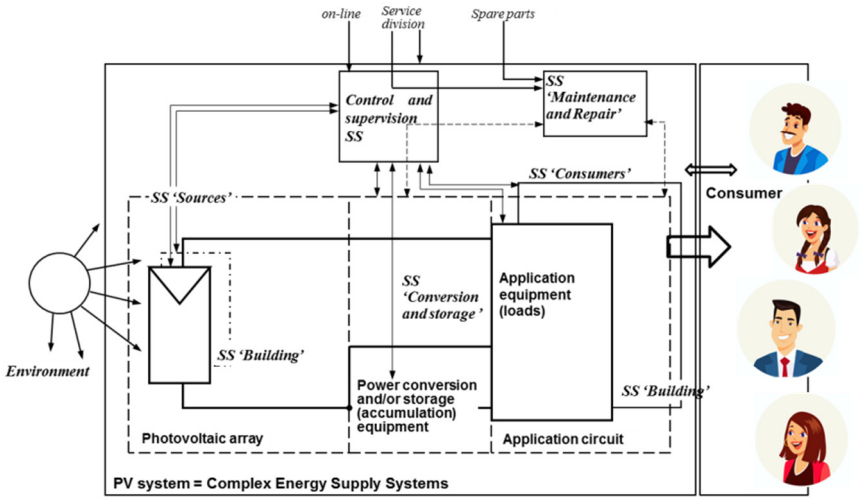

Figure 10. Design of highly efficient PV system for individual facilities created as a complex system of energy supply to the facility (SS means "subsystem").

Unlike ordinary network systems, the problem of the interconnection of all processes, from power production to power consumption, is critically important for PV systems. If a system is improperly organized or its structure is not optimized, there will be an energy shortage, or even an absence of energy supply, on the consumer side. It is obvious that in particular cases, the assertions of inapplicability (inoperability) of a PV system or its lower efficiency compared with the expected values of parameters, are, first of all, associated with improper organization and structure of the PV system. When a PV system is used for power supply to a facility, its maximum efficiency may only be achieved when it is designed in accordance with the foregoing principles.

The efficiency criterion of highly efficient PV systems is formulated as follows: "maximum satisfaction of needs with minimum costs", and the objective function, generally, is as follows:

$$W = \begin{cases} \mathrm{S} \to \max \\ \mathrm{C_E} \to \min \\ HE \to 0 \end{cases} \tag{9}$$

Provided that

$$(\mathrm{C_E} \to \min) \equiv \left\{ \begin{array}{l} E_{\mathrm{cn}} \to \min \\ EL_{\Sigma} = EL_1 + EL_2 + EL_3 + EL_4 + EL_5 + EL_6 \to \min \end{array} \right\} \tag{10}$$

$$(E_{\mathrm{cn}} \to \min) \equiv \left\{ \begin{array}{l} E_{\mathrm{d}} \to \min \\ EL_6 \to \min \end{array} \right\} \tag{11}$$

$$(E_{\mathrm{d}} \to \min) \supset \begin{Bmatrix} \text{Need optimization/correct assessment of needs} \\ \text{Consumption equipment optimization} \end{Bmatrix} \tag{12}$$

where S is the degree of need satisfaction (if S is expressed as a percentage, then $S \to 100\%$); C_{E} is the energy expenditure; HE is the environmental damage; EL_{d} is the energy demand; and EL_{Σ} is the aggregate energy losses. E_{cn}, EL_1, EL_2, EL_3, EL_4, EL_5, and EL_6 are shown in Figure 9.

With that, the cost minimization is assumed to be, first and foremost, the minimization of energy expenditures and, therefore, the minimization of losses. Additionally, the maximum satisfaction of needs is understood to be the maximum number of needs met and the maximum satisfaction of each need. Methods for numeric evaluation at the level of individual facilities do not yet exist for all the indices through which the needs are expressed. In this case, one proceeds from the affirmation that a greater observance of this condition corresponds to greater satisfaction of needs and is always preferable, e.g., more ecologically sound solutions are always preferable.

The correct assessment and formalization of needs is the most difficult task in the creation of PV systems in accordance with the proposed efficiency criterion in Equation (9). This occurs in the following manner:

The consumer is described by a set of needs N for the satisfaction of which electrical energy (or electrical energy from a PV system) may be required. Each need n_i is described from 1 to J by parameters p_{ij}. In a general case, the number of parameters characteristic of different needs is different. Each of the parameters is characterized by a value (or permissible value range) of v_{ij} corresponding to the state of "need is satisfied", or a number of values/ranges and the relevant degrees of need satisfaction are established for each parameter. The general outline of consumer need formalization may be presented through the following identical relations:

$$\text{Consumer} \equiv \begin{Bmatrix} \textit{Set} \\ \textit{of needs} \\ \mathrm{N} \\ \mathrm{N} = \{n_1, n_2, \ldots, n_i\} \end{Bmatrix} \Leftrightarrow \begin{Bmatrix} \textit{Set} \\ \textit{of the parameters} \\ \textit{characterizing} \\ \textit{needs} \\ \mathrm{NP} \\ \mathrm{NP} = \begin{Bmatrix} \{\mathrm{NP}_1\} \\ \{\mathrm{NP}_2\} \\ \ldots \\ \{\mathrm{NP}_i\} \end{Bmatrix} \end{Bmatrix} \equiv \begin{vmatrix} \mathrm{NP}_1 = \{p_{11}, p_{12}, \ldots, p_{1j}\} \\ \mathrm{NP}_2 = \{p_{21}, p_{12}, \ldots, p_{2j}\} \\ \ldots \\ \mathrm{NP}_i = \{p_{i1}, p_{i2}, \ldots, p_{ij}\} \end{vmatrix} \Leftrightarrow \begin{Bmatrix} \textit{Set} \\ \textit{of the parameter} \\ \textit{values} \\ \textit{characterizing} \\ \textit{needs} \\ \mathrm{NPV} \\ \mathrm{NPV} = \begin{Bmatrix} \{\mathrm{NPV}_1\} \\ \{\mathrm{NPV}_2\} \\ \ldots \\ \{\mathrm{NPV}_i\} \end{Bmatrix} \end{Bmatrix} \equiv \begin{vmatrix} \mathrm{NPV}_1 = \{v_{11}, v_{12}, \ldots, v_{1j}\} \\ \mathrm{NPV}_2 = \{v_{21}, v_{12}, \ldots, v_{2j}\} \\ \ldots \\ \mathrm{NPV}_i = \{v_{i1}, v_{i2}, \ldots, v_{ij}\} \end{vmatrix} \tag{13}$$

where NP is the set of parameters characterizing all consumer needs that require electrical energy to be met, NP_i is the set of the parameters characterizing the i-th need, NPV is the set of the parameter values characterizing all needs, and NPV_i is the set of parameter values characterizing the i-th need.

The task of creating a PV system is to ensure that the energy generated by it meets each need. Formally, this means that the value of each parameter from the set of parameters in Equation (13) is equal to the desired value (i.e., it is within the desired range of values).

The process that is fully applied today is shown in Figure 11. The system efficiency evaluation is carried out in reverse order.

Additionally, the efficiency of such PV systems is as follows:

$$\eta_{\mathrm{syst}} = \frac{E_{\mathrm{cn}} - \Delta_E}{E_{\mathrm{in}}} \cdot 100\% \tag{14}$$

where E_{in} is the amount of energy supplied to the system (the product of the aggregate irradiance of PV module active surfaces or CPV module aperture by the aggregate area of active surfaces or aperture). In the case of power supply with the use of PV systems,

these are only $E_{in} = E_{cn} + (EL_{PV} + EL_3 + EL_4 + EL_5 + EL_6)$; $EL_{PV} = EL_1$ is the losses in the generation process; and Δ_E is the difference between the energy required for consumer needs to be fully met and the clean energy directly used to meet consumer needs.

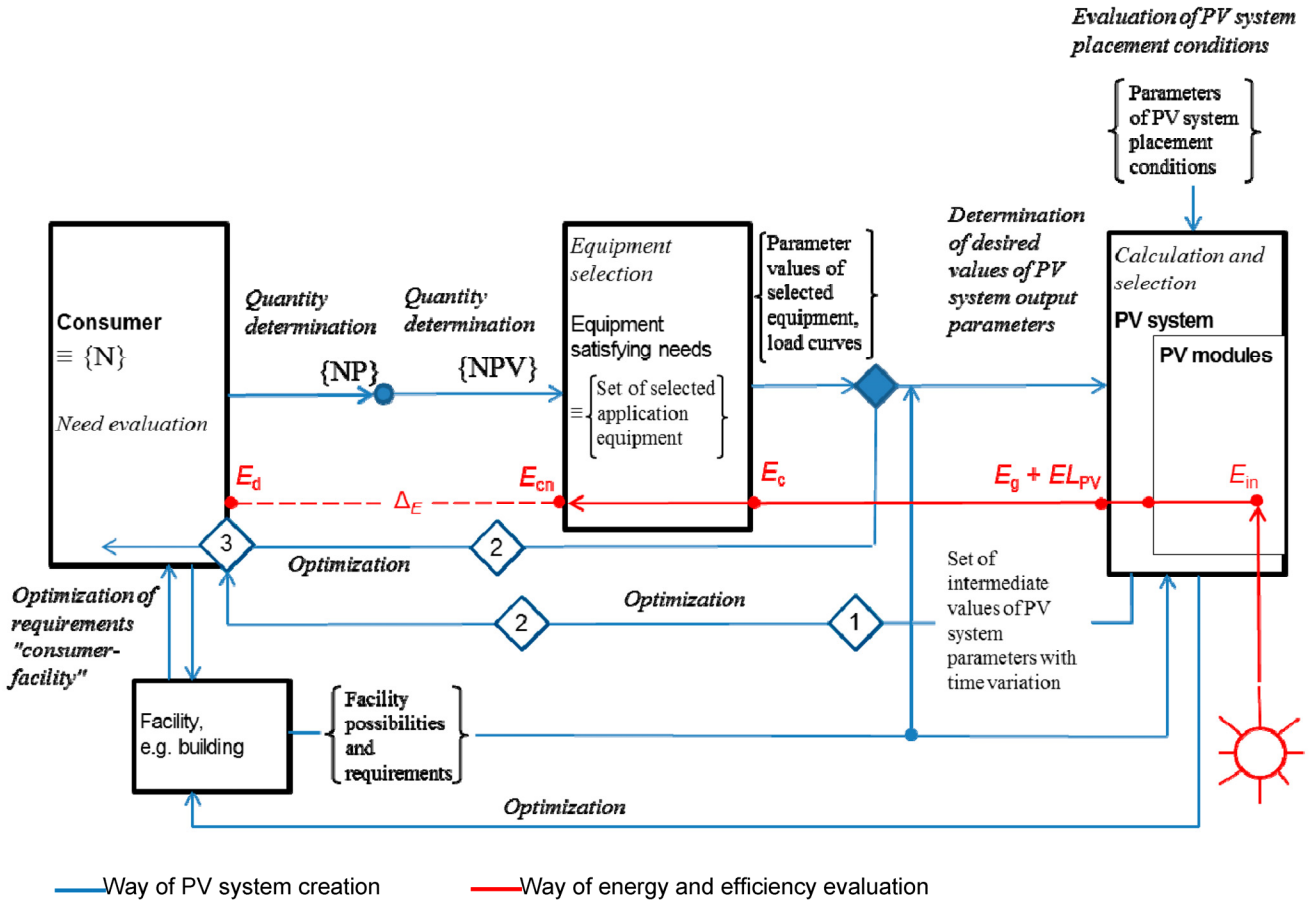

Figure 11. Diagram of PV system implementation and its efficiency evaluation.

Instead of energy, power may be used to simplify the evaluation process. In this case, to assess the efficiency, instead of Δ_E, it is necessary to determine Δ_P, which is the total power of all needs that are not fully met.

The efficiency evaluation according to the proposed criterion and the creation of a PV system in accordance with Figure 10 indispensably include the possibility of amendments, adjustments, and modifications as a normal functional condition of the process, from changing settings to the replacement of equipment, software logic, etc. This includes the possibility of modifications due to the inaccurate assessment of the state of need satisfaction resulting from (1) PV system's imperfection due to any errors in design and inaccurate determination of the consumer needs from the outset as well as (2) a change in needs.

The described approach may be quite properly combined with modern software possibilities, which allows for the implementation of the diagram in Figure 11 in practice.

5. Approbation of Proposed Solutions

The final characteristics of the developed PV/CPV modules, as well as typical average characteristics of conventional mono-Si modules, are shown in Table 3. As can be seen from the *I–V* curve of the developed modules (Figures 2c, 5b, 7b and 8c), it is possible to

further increase the PV/CPV modules' efficiency, especially the modules based on planar high-voltage PV cells.

Table 3. Characteristics of the newly developed PV/CPV modules and typical characteristics of conventional crystalline Si PV modules.

Module Type	Active Surface or Aperture (mm)	Height (mm)	$V_{o.c}$ (V)	$J_{s.c}$ (mA/sm^2)	V_{mpp} (V)	J_{mpp} (mA/sm^2)	P_{max} (W/sm^2)
Conventional crystalline Si PV modules (60 single *p*–*n* junction mono-Si PV cells with size 156.75 × 156.75 mm)	1671.0 × 1002.0	35.0	44.0	0.567	36.3	0.526	0.019
PV module-based vertical high-voltage PV cells	60.0 × 10.0	0.4	640.0 [1]	0.559 [1]	548.5 [1]	0.456 [1]	0.250 [1]
PV module-based planar high-voltage PV cells	1578.5 × 945.5	37.1	439.7	0.0625	382.4	0.061	0.023
CPV module-based one-dimensional double-wing concentrator and vertical high-voltage PV cells (one section)	37.64 × 1020.0	75.4	730.0	0.0453	637	0.038	0.024
CPV module-based multi-zone microconcentrator and planar high-voltage PV cells	1607.0 × 967.4	47.2	512.9	0.068	405.0	0.058	0.023

[1] Under 10 suns.

In the period from 2011 to 2022, the concept considered above was used for designing PV systems in various climate conditions and at facilities with different needs [43,60–64]. The functioning of those systems confirms the correctness of the proposed approach. The composed systems can satisfy 30–50% more needs than PV systems with a conventional systematization level simultaneously installed at similar facilities, i.e., they are equivalent to PV systems with a conventional systematization level but generate more energy by 30–50%. The points of PV systems' installation were in various regions of rural territories with different climates, so the results may be deemed quite representative.

The research results presented in Sections 2–4 were combined in the base experimental project of an ecological complex (Lat 58.01 N, Lon 43.34 E) consisting of two main buildings and free-standing identical cottages whose number grew from year to year. The PV system was implemented from the outset as a comprehensive power supply system with conventional mono-Si PV modules located on the roof and integrated into the balcony rail and flexible a-Si panels on the roof with an arched form [60]. As new PV/CPV modules were developed, these new devices would be partially installed for conventional planar modules. The power supply to one of the cottages, in comparison, was ensured from the very beginning using a conventional PV system. The rest were designed with a different higher level of systematization. Depending on the particular cottage, the systematization level increased with the extension options by incorporating into the system other components involved in the power supply process (see Figures 8 and 9). Additionally, the level of systematization of parts of the PV system of the main buildings was gradually adjusted.

Thanks to the installation of the developed PV and CPV modules, the total maximum power at STC (CSTC) was 1120.86 kW. That said, thanks to a higher output voltage and other specific features of the modules, the losses inside the system decreased by 12 to 15%, and also maintenance losses decreased. In the case of PV systems of the cottages built simultaneously with the cottage equipped with a traditional PV system, the power directly used to meet consumer needs was 21% to 23% higher. As the proposed approach was improved, in the construction of new cottages, losses were reduced, and E_{cn} was increased by 12% to 16%.

The reduction values of the maximum power at STC/CSTC, and, consequently, those of the energy production of the developed PV modules, were from 0.2% to 0.24% per year under wet atmospheres with high concentrations of dissolved ammonia (see Figure 12). These values of the developed PV modules were from 0.22% to 0.37% per year. Measurements

were carried out on a livestock complex experimental site and using an accelerated aging method in laboratory conditions. For comparison reasons, Figure 12 shows the deterioration range for conventional mono-Si PV modules, in a normal environment. The average annual deterioration of their performance may attain 5% to 7%, in a wet ammonia environment.

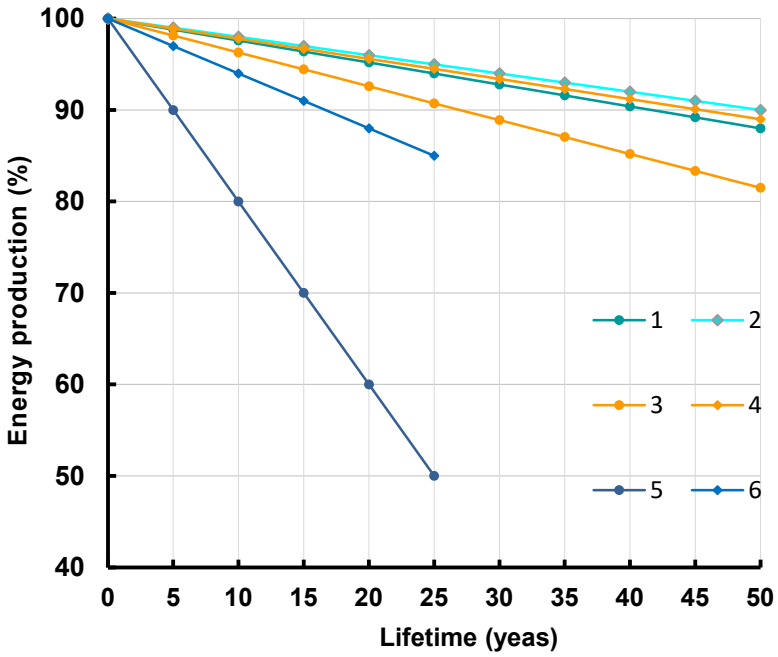

Figure 12. Reduction in the energy production of modules during their operation lifespan: 1, 2—newly developed PV modules with high-voltage PV cells in wet ammonia environment (1—maximum, 2—minimum); 3, 4—newly developed CPV modules in wet ammonia environment (3—maximum, 4—minimum); 5, 6—conventional mono-Si PV modules in normal operation conditions (5—maximum, 6—minimum).

6. Conclusions

The use of PV equipment is a real efficient method for fighting against climate change, and the protection and restoration of the environment. For the mass implementation of PV systems in agriculture in rural areas, their attractiveness to consumers should be increased, for which it is necessary to improve the energy output of PV devices, as well as their reliability and environmental resistance, to improve their aesthetic quality, as well as enhance the diversity of efficient PV equipment for any operational conditions ensuring the versatility of PV systems use as an energy source.

High-voltage vertical Si PV cells for terrestrial applications and high-voltage multi-junction planar Si PV cells were proposed and developed. A significant increase in the output voltage of the PV modules and PV arrays was attained with the design of PV cells that enabled a reduction in power losses, material consumption, required space, and cost. At the same time, the design of planar multijunction PV cells allowed for adherence to the conventional mass production technology for PV modules.

The modules based on high-voltage vertical PV cells composed of 40 cells had a size of 60 × 10 mm, a maximum power point voltage of up to 1000 V, specific power of up to 0.245 ± 0.01 W/cm^2, and an efficiency rate of up to 25.3%, for radiation concentration ratios from 10 to 100. The samples of the second type of modules composed of 60 PV cells (156.75 × 156.75 mm) had $V_{o.c}$ = 439.7 V, $I_{s.c}$ = 0.933 A, and P_{max} of 348 W, at STC. The maximum power degradation at STC was estimated to be within 0.2% to 0.24% per year in a wet ammonia environment.

New designs of concentrators with uniform radiation distribution in the focal region were developed, including a parabolic cylindrical concentrator with minimized Fresnel

optical losses and a multi-zone parabolotoric microconcentrator whose dimensions enabled CPV modules similar in size to conventional planar modules to be manufactured. Two types of CPV modules were designed: (1) modules consisting of a parabolic cylindrical concentrator and an RR composed of vertical multi-junction cells, and (2) modules comprising multi-zone microconcentrators with a planar high-voltage multi-junction cell as the RR. The second-type CPV modules included 42 × 29 microconcentrators and had the dimensions of 1607.8 × 967.4 ×47.2 mm. These modules had the following average values of output parameters at CSTC: $V_{o.c}$ = 512.9 V, $I_{s.c}$ = 1.051 A, and P_{max} of 361.57 W. The degradation of maximum power at CSTC was estimated at 0.22% to 0.37% per year in a wet ammonia environment.

Through the use of PV and CPV modules based on the developed cells and concentrators, projects using the power supply on the basis of PV systems were designed. The projects implemented the principles of complex energy supply systems, which allowed for the minimization of the losses and requirements for the output power level of PV systems. The thus-created systems satisfied 30–50% more consumer needs than PV systems with a traditional systematization level simultaneously installed at similar facilities. Thanks to a higher output voltage and other specific features of the developed modules, the power loss inside the PV system decreased by 12% to 15%, along with a reduction in maintenance loss.

Author Contributions: Conceptualization, O.S.; methodology, O.S.; validation, O.S., A.I., Y.L. and A.D.; formal analysis, O.S.; investigation, O.S.; resources, A.I., Y.L. and A.D.; data curation, A.I., Y.L., and A.D.; writing—original draft preparation, writing—review and editing, O.S.; visualization, O.S. and A.D.; supervision, A.I., Y.L. and A.D.; project administration, A.I., Y.L. and A.D.; funding acquisition, A.I, Y.L. and A.D. All authors have read and agreed to the published version of the manuscript.

Funding: This research received no external funding.

Institutional Review Board Statement: Not applicable.

Data Availability Statement: Not applicable.

Conflicts of Interest: The authors declare no conflict of interest.

References

1. Konovalov, S.S. *Man and the Universe*; AST: Moscow, Russia, 2022.
2. Barron-Gafford, G.A.; Pavao-Zuckerman, M.A.; Minor, R.L.; Sutter, L.F.; Barnett-Moreno, I.; Blackett, D.T.; Thompson, M.; Dimond, K.; Gerlak, A.K.; Nabhan, G.P.; et al. Agrivoltaics provide mutual benefits across the food–energy–water nexus in drylands. *Nat. Sustain.* **2019**, *2*, 848–855. [CrossRef]
3. Weselek, A.; Bauerle, A.; Hartung, J.; Zikeli, S.; Lewandowski, I.; Högy, P. Agrivoltaic system impacts on microclimate and yield of different crops within an organic crop rotation in a temperate climate. *Agron. Sustain. Dev.* **2021**, *41*, 59. [CrossRef]
4. Ghosha, S.; Ranjana Yadav, R. Future of photovoltaic technologies: A comprehensive review. *Sustain. Energy Technol. Assess.* **2021**, *47*, 101410. [CrossRef]
5. Elahi, E.; Khalid, Z.; Zhang, Z. Understanding farmers' intention and willingness to install renewable energy technology: A solution to reduce the environmental emissions of agriculture. *Appl. Energy* **2022**, *309*, 118459. [CrossRef]
6. Izmailov, A.Y.; Lobachevsky, Y.P.; Shepovalova, O.V. Solar power systems implementation potential for energy supply in rural areas of Russia. *AIP Conf. Proc.* **2019**, *2123*, 020104. [CrossRef]
7. Ufa, R.A.; Malkova, Y.Y.; Rudnik, V.E.; Andreev, M.V.; Borisov, V.A. A review on distributed generation impacts on electric power system. *Int. J. Hydrogen Energy* **2022**, *47*, 20347–20361. [CrossRef]
8. Shepovalova, O.V. Specificity of the individual energy supply systems creation in Russia. In Proceedings of the 42nd ASES National Solar Conference SOLAR 2013, Including 42nd ASES Annual Conference and 38th National Passive Solar Conference, Baltimore, MD, USA, 16–20 April 2013.
9. Hafeez, M.; Yuan, C.; Shah, W.U.; Mahmood, M.T.; Li, X.; Iqbal, K. Evaluating the relationship among agriculture, energy demand, finance and environmental degradation in one belt and one road economies. *Carbon Manag.* **2020**, *11*, 139–154. [CrossRef]
10. Vasiliev, A.M.; Landsman, A.P. *Semiconductor Photoelectric Converters*; Soviet Radio Pupl.: Moscow, Russia, 1971.
11. Arbuzov, Y.D.; Evdokimov, V.M. *Fundamentals of Photovoltaics*; GNU VIESH: Moscow, Russia, 2008.
12. Dhilipan, J.; Vijayalakshmi, N.; Shanmugam, D.B.; Jai Ganesh, R.; Kodeeswaran, S.; Muralidharan, S. Performance and efficiency of different types of solar cell material—A review. *Mater. Today Proc.* **2022**, *66*, 1295–1302. [CrossRef]

13. Fraunhofer Institute for Solar Energy Systems (ISE) with Support of PSE Projects GmbH. *Photovoltaics Report*; Fraunhofer ISE FHG-SK—ISE-PUBLIC: Freiburg, Germany, 2023. Available online: https://www.ise.fraunhofer.de/content/dam/ise/de/documents/publications/studies/Photovoltaics-Report.pdf (accessed on 26 March 2023).
14. Strebkov, D.S.; Tver'yanovich, E.V. *Concentrator of Solar Radiation*; GNU VIESH: Moscow, Russia, 2007.
15. *Integrated Photovoltaics—Areas for the Energy Transformation*; Fraunhofer ISE: Freiburg, Germany, 2023. Available online: https://www.ise.fraunhofer.de/en/key-topics/integrated-photovoltaics.html (accessed on 26 March 2023).
16. Mamun, M.Z.; Dargusch, P.; Wadley, D.A.; Zulkarnain, N.A.; Aziz, A.A. A review of research on agrivoltaic systems. *Renew. Sustain. Energy Rev.* **2022**, *161*, 112351. [CrossRef]
17. Izmailov, A.Y.; Lobachevsky, Y.P.; Shepovalova, O.V. Complex energy supply systems for individual sites. *Energy Procedia* **2019**, *157*, 1445–1455. [CrossRef]
18. Shepovalova, O.V. Mandatory Characteristics and Parameters of Photoelectric Systems, Arrays and Modules and Methods of their Determining. *Energy Procedia* **2019**, *157*, 1434–1444. [CrossRef]
19. Green, M.A.; Dunlop, E.D.; Siefer, G.; Yoshita, M.; Kopidakis, N.; Bothe, K.; Hao, X. Solar cell efficiency tables (Version 61). *Prog. Photovolt. Res. Appl.* **2022**, *31*, 3–16. [CrossRef]
20. Bagher, A.M.; Vahid, M.M.A.; Mohsen, M. Types of solar cells and application. *Am. J. Opt. Photon.* **2015**, *3*, 94–113. [CrossRef]
21. Würfel, P.; Würfel, U. *Physics of Solar Cells: From Principles to New Concepts*, 3rd ed.; Wiley-VCH: Weinheim, Germany, 2009.
22. Morocha, A.K. On the theory of love waves in heterostructures with hexagonal symmetry. *Semiconductors* **2010**, *44*, 1625–1630. [CrossRef]
23. Strebkov, D.S. *Matrix Solar Cells*; GNU VIESH: Moscow, Russia, 2010; Volume I–III.
24. Xing, Y.; Han, P.; Wang, S.; Fan, Y.; Liang, P.; Ye, Z.; Li, X.; Hu, S.; Lou, S.; Zhao, C.; et al. Performance analysis of vertical multi-junction solar cell with front surface diffusion for high concentration. *Sol. Energy* **2013**, *94*, 8–18. [CrossRef]
25. Arbuzov, Y.D.; Evdokimov, V.M.; Strebkov, D.S.; Shepovalova, O.V. Semiconductor Photoelectric Generator (Versions) and Method of Making Said Generator (Versions). R.F. Patent 2371811, 27 October 2009.
26. Arbuzov, Y.D.; Evdokimov, V.M.; Strebkov, D.S.; Shepovalova, O.V. Semiconductor Photoelectric Generator and Method of Making Said Generator. R.F. Patent No. 2373607, 20 November 2009.
27. Arbuzov, Y.D.; Evdokimov, V.M.; Shepovalova, O.V. Cascade photoconverters on the basis of the homogeneous semiconductor tunnel structures. In Proceedings of the World Renewable Energy Forum, WREF 2012, Including World Renewable Energy Congress XII and Colorado Renewable Energy Society (CRES) Annual Conference, Denver, CO, USA, 13–19 May 2012; Volume 1, pp. 147–153.
28. Arbuzov, Y.D.; Evdokimov, V.M.; Shepovalova, O.V. Spectral characteristics of cascade photoelectric converters on the base of idealized tunnel homogeneous semiconductor structures. *AIP Conf. Proc.* **2018**, *1968*, 030007. [CrossRef]
29. Arbuzov, Y.D.; Evdokimov, V.M.; Majorov, V.A.; Saginov, L.D.; Shepovalova, O.V. Silicon PV Cell Design and Solar Intensity Radiation Optimization for CPV Systems. *Energy Procedia* **2015**, *74*, 1543–1550. [CrossRef]
30. Arbuzov, Y.D.; Evdokimov, V.M.; Shepovalova, O.V. New Photoelectric System on the Basis of Cascade Homogeneous Photoconverters and Solar Radiation Concentrators. *Energy Procedia* **2015**, *74*, 1533–1542. [CrossRef]
31. Vasiliev, A.M.; Evdokimov, V.M.; Landsman, A.P.; Milovanov, A.F. Operation of photoconverters under conditions of strong illumination. *Geliotekhnika* **1975**, *11*, 72–87.
32. Khamooshi, M.; Salati, H.; Egelioğlu, F.; Faghiri, A.H.; Tarabishi, J.; Babadi, S. A Review of Solar Photovoltaic Concentrators. *Int. J. Photoenergy* **2014**, *2014*, 1–17. [CrossRef]
33. Wang, L.; Yuan, Z.; Zhao, Y.; Guo, Z. Review on Development of Small Point-Focusing Solar Concentrators. *J. Therm. Sci.* **2019**, *28*, 929–947. [CrossRef]
34. Almonacid, G.; Lique, A.; Moledo, A.G. Photovoltaic static concentrator analysis. *Sol. Cells* **1984**, *1*, 163–178. [CrossRef]
35. Li, G.; Xuan, Q.; Akram, M.W.; Akhlaghi, Y.G.; Liu, H.; Shittu, S. Building integrated solar concentrating systems: A review. *Appl. Energy* **2020**, *260*, 114288. [CrossRef]
36. Shanks, K.; Senthilarasu, S.; Mallick, T.K. Optics for concentrating photovoltaics: Trends, limits and opportunities for materials and design. *Renew. Sustain. Energy Rev.* **2016**, *60*, 394–407. [CrossRef]
37. Zahidov, R.A.; Umarov, G.Y.; Vainer, A.A. *Theory and Calculating Helio-Technical Concentrating Systems*; FAN: Tashkent, Russia, 1977.
38. Paul, D.I. Application of compound parabolic concentrators to solar photovoltaic conversion: A comprehensive review. *Int. J. Energy Res.* **2019**, *43*, 4003–4050. [CrossRef]
39. Li, G.; Xuan, Q.; Pei, G.; Su, Y.; Ji, J. Effect of non-uniform illumination and temperature distribution on concentrating solar cell—A review. *Energy* **2018**, *144*, 1119–1136. [CrossRef]
40. Alves, M.; Pérez-Rodríguez, A.; Dale, P.J.; Domínguez, C.; Sadewasser, S. Thin-film micro-concentrator solar cells. *J. Phys. Energy* **2020**, *2*, 012001. [CrossRef]
41. AL-Hamadany, A.H.; Al-Abideen, F.S.Z.; Ali, J.H. Effect of Angle Orientation of Flat Mirror Concentrator on Solar Panel System Output. *IOSR J. Comput. Eng.* **2016**, *18*, 16–23.
42. Vu, N.H.; Pham, T.T.; Shin, S. Large Scale Spectral Splitting Concentrator Photovoltaic System Based on Double Flat Waveguides. *Energies* **2020**, *13*, 2360. [CrossRef]
43. Shepovalova, O.V.; Izmailov, A.Y.; Lobachevsky, Y.P.; Dorokhov, A.S.; Chirkov, S.V. Solar energy toroidal concentrators. *Energy Rep.* **2021**, *7*, 328–342. [CrossRef]

44. Shepovalova, O.V. Fabrication process study for matrix silicon solar cells. *AIP Conf. Proc.* **2017**, *1814*, 020077. [CrossRef]
45. Strebkov, D.S.; Shepovalova, O.V.; Bobovnikov, N.I. Investigation of High-Voltage Silicon Solar Modules. *AIP Conf. Proc.* **2019**, *2123*, 020103. [CrossRef]
46. Strebkov, D.S.; Shepovalova, O.V.; Zadde, V.V. Semiconductor Photoelectric Generator. R.F. Patent 2336596, 20 October 2008.
47. Wheeler, N.R.; Bruckman, L.S.; Ma, J.; Wang, E.; Wang, C.K.; Chou, I.; Sun, J.; French, R.H. Degradation pathway models for photovoltaics module lifetime performance. In Proceedings of the IEEE 39th Photovoltaic Specialists Conference (PVSC), Tampa, FL, USA, 16–21 June 2013; pp. 3185–3190. [CrossRef]
48. Poulek, V.; Strebkov, D.S.; Persic, I.S.; Libra, M. Towards 50 years lifetime of PV panels laminated with silicone gel technology. *Sol. Energy* **2012**, *86*, 3103–3108. [CrossRef]
49. *IEC 61215-2:2021*; Terrestrial Photovoltaic (PV) Modules—Design Qualification and Type Approval—Part 2: Test Procedures. International Electrotechnical Commission: Geneva, Switzerland, 2021.
50. *IEC/TS 63126:2020*; Guidelines for Qualifying PV Modules, Components and Materials for Operation at High Temperatures. International Electrotechnical Commission: Geneva, Switzerland, 2020.
51. *IEC 62716:2013*; Photovoltaic (PV) Modules—Ammonia Corrosion Testing. International Electrotechnical Commission: Geneva, Switzerland, 2013.
52. *IEC 61701:2020*; Salt Mist Corrosion Testing of Photovoltaic (PV) Modules. International Electrotechnical Commission: Geneva, Switzerland, 2020.
53. Arbuzov, Y.D.; Evdokimov, V.M.; Shepovalova, O.V. Multi-zone parabolotoric micro-concentrator of solar energy. *AIP Conf. Proc.* **2019**, *2190*, 020093. [CrossRef]
54. Tabunschikov, Y.A.; Brodach, M.M.; Shilkin, N.V. *Energy-Efficient Buildings*; AVOK–PRESS: Moscow, Russia, 2013.
55. Iturriagaa, E.; Aldasoro, U.; Campos-Celadorc, A.; Sala, J.M. A general model for the optimization of energy supply systems of buildings. *Energy* **2017**, *138*, 954–966. [CrossRef]
56. Petri, I.; Kubicki, S.; Rezgui, Y.; Guerriero, A.; Li, H. Optimizing Energy Efficiency in Operating Built Environment Assets through Building Information Modeling: A Case Study. *Energies* **2017**, *10*, 1167. [CrossRef]
57. *IEC/TS 62257-9-6:2019*; Recommendations for Small Renewable Energy and Hybrid Systems for Rural Electrification—Part 9–6: Integrated System—Selection of Photovoltaic Individual Electrification Systems (PV-IES). International Electrotechnical Commission: Geneva, Switzerland, 2019.
58. *IEC 62548:2016*; Photovoltaic (PV) Arrays—Design Requirements. International Electrotechnical Commission: Geneva, Switzerland, 2016.
59. Izmailov, A.Y.; Lobachevsky, Y.P.; Shepovalova, O.V. Comparison and selection of off-grid PV systems. *AIP Conf. Proc.* **2018**, *1968*, 030001. [CrossRef]
60. Strbkov, D.S.; Shepovalova, O.V.; Dunichkin, I.V. Energetically independent buildings of the resort-improving and educational-recreational complex in ecological settlement "GENOM". In Proceedings of the World Renewable Energy Forum, WREF 2012, Including World Renewable Energy Congress XII and Colorado Renewable Energy Society (CRES) Annual Conference, Denver, CO, USA, 13–19 May 2012; pp. 3767–3772.
61. Dunichkin, I. Aspects of designing construction of balcony parapets with photoelectric cells. *MATEC Web Conf.* **2016**, *86*, 02014. [CrossRef]
62. Dorokhov, A.S.; Shepovalova, O.V. Solar PV systems integrated into hardscape and sculptures. *AIP Conf. Proc.* **2019**, *2190*, 020094. [CrossRef]
63. Shepovalova, O.V.; Kondratenko, P.N. Complex power supply systems for agricultural facilities based on PV systems. In Proceedings of the International Scientific Conference "Prospects for the Development of Agriculture Energy Supply", Tomsk, Russia, 26–30 March 2020; pp. 25–37.
64. Noborov, P.R.; Barentzov, Y.I.; Kondratenko, P.N. PV systems integrated into barn buildings. In Proceedings of the Scientific Conference "Agriculture and Future", Krasnodar, Russia, 8–9 June 2021; pp. 118–127.